

Modeling and Observer Design of a Nonlinear LCL Filter for Three- Phase Grid-Connected Voltage Source Converter

Taravat Saryan



LUND
UNIVERSITY

Department of Automatic Control

Msc Thesis
ISRN LUTFD2/TFRT--5938--SE
ISSN 0280-5316

Department of Automatic Control
Lund University
Box 118
SE-221 00 LUND
Sweden

© 2014 by Taravat Saryan. All rights reserved.
Printed in Sweden by Media-Tryck
Lund 2014

Abstract

This work presents an observer design for grid current and capacitor voltage of voltage source pulse-width modulation (PWM) converters with LCL filter. Theoretical aspects including the mathematical LCL filter system observability, observer placement strategy and practical discretization implementation. It gives insight to mathematical modelling of the line filters dynamics. By the limitations of how the components in the line filter operates, the Kalman filter is adjusted accordingly.

The strategy for designing the Kalman filter is presented. A time-varying KF is developed, benchmarked and implemented in simulator.

Through an explanation of the magnetic field fundamentals, a nonlinear model of the inductors is modeled and used. An observer scheduling development has been implemented on the nonlinear system. The effect of sampling frequency is studied for KF and for the observer as well. At last the results are presented and analyzed.

Acknowledgements

I sincerely thank the supervisor Prof. Dr. Rolf Johansson from Lund University for his valuable guidance during the course of my thesis work and I would like to thank Nils Lundström from Comsys AB, for his ever enthusiastic supervision and motivating guidance. I express my appreciation for the patience and understanding each one of them have shown towards me. Their timely suggestions have been of great help in leading me to the completion of my Master thesis.

I thank my mother and father for their unconditional support and for being my source of the strength. I thank my friends for their care and understanding.

Lund University
April 24, 2014

Taravat Saryan

Contents

1. Introduction.....	7
1.1 Background.....	7
1.2 Project Motivation	9
1.3 Problem Formulation	10
1.4 Outline of the Project.....	10
2. Line Filters Topology	12
2.1 Line Filter	12
3. Mathematical Model and Transfer functions for LCL Filters.....	14
3.1 Background.....	14
3.2 Mathematical Model Including Stray Resistor.....	15
4. Inductor.....	18
4.1 Introduction.....	18
4.2 Inductor Characteristics	18
4.3 Modeling Nonlinear Inductors.....	20
5. Simulation Results	24
5.1 Simulation Model for Linear LCL Filter	24
5.2 Modeling the Nonlinear Inductance under Matlab/Simulink.....	24
6. Observer Algorithm and Parameters.....	31
6.1 Theoretical Formulation of the Kalman Filter	31
6.2 General Information.....	32

6.3 Kalman Observer Design for LCL Filter	33
6.4 Observer Scheduling	38
6.5 Scheduling Approaches	39
7. MATLAB/Simulink Result.....	41
7.1 Experimental setup.....	41
7.2 Simulation for Linear System Dynamics	45
7.3 Simulation for Nonlinear System Dynamics.....	56
8. References.....	64

1. Introduction

This chapter starts by describing the company background and the company's product, an Active Dynamic Filter (ADF), next, the motivation of the thesis and an overview of the problem is presented. Finally, the outline of the thesis is presented.

1.1 Background

Energy consumption has increased drastically in both industrialized and developing countries and it is predicted to continue increasing. Technological innovation will play a central role by improving energy efficiency. Comsys AB is one of the companies which have a vision to provide the knowledge and equipment needed for minimizing energy consumption. Comsys AB has focused on finding solutions for improving power quality. The term power quality can be described as a set of values of parameters and disturbances that cause deviations from pure sinusoidal waveform in an Alternating Current (AC) system [35]. The most well-known disturbances are harmonics connected in the sinus waveform for AC power, frequency variations, voltage unbalances and transients. These disturbances may cause significant loss of performance and life time of equipment etc.

Comsys AB has developed a product that can overcome these kinds of problems and thereby improve energy efficiency. The product is an active filter called Active Dynamic Filter (ADF). An active filter can compensate almost any power quality issues. There are several different ADF models. These models differ from each other depending on their compensation current capacity.

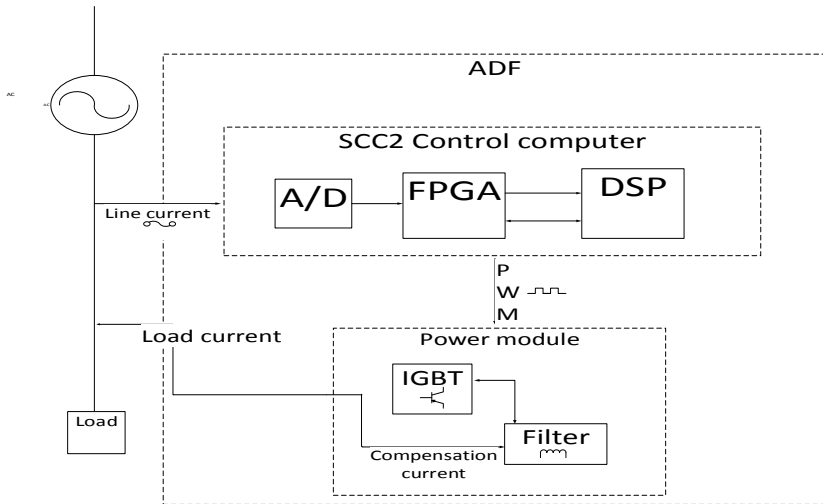


Fig. 1.1 Block diagram of an ADF

The main components of ADF are:

- **Power converter:** the converter that is used in ADFs consist of a DC-link to store energy, an Insulated-Gate Bipolar Transistor (IGBT) and a Back Charging (BC) board
- **Line filter (LCL):** LCL filters have several tasks to do such as: decouple energy between grid-connected voltage source converters, attenuate current ripple, filter differential mode and common mode inverter switching noise[2], make it possible to create arbitrary current needed to counteract the measured disturbances, etc. [35]
- **Computer control:** Sniff Computer Control (SCC2) is an advanced stand-alone real time control system for distributed three phase power converter control in ADF compensation applications.

SCC2 consist mainly of:

1. An A/D converter that reads the voltage value and converts it to the digital value which is fetched by the Field Programmable Gate Array (FPGA)

2. FPGA supports the DSP by controlling/sampling A/D conversion and generating Pulse Width Modulation (PWM) pulses. FPGA is running at 60MHz.
3. Digital Signal Processor (DSP) is running the high-level code, i.e. control loop and communications and it is the master of the system. It is a fixed point 32bit processor running at 600MHz, named Blackfin as well.

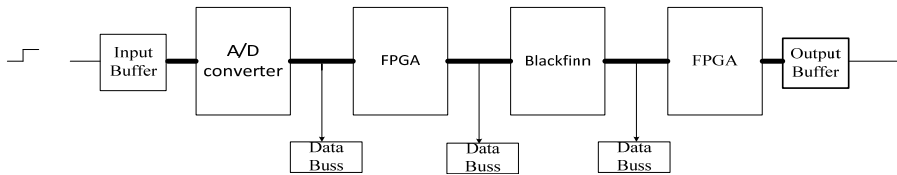


Fig. 1.2 A simplified block structure of the SCC2

1.2 Project Motivation

Many systems in nature are nonlinear [41]. Some control methods that have been developed for nonlinear plants approximate the nonlinearity as linear. However, the linearization methods may fail if the system is highly nonlinear. The nonlinearities that are of interest for this thesis are those belonging to the components in the LCL filter. The inductance values decrease with increasing current through them, since the inductors are non-ideal. It would be more beneficial, both from a technical and a usability point of view, to have a design where the non-linearity of the components is taken into consideration [35]. A system with this new model design would optimize future control algorithms and lead to decreased model faults. A system with these properties can also be realized by control observer design and modeling. These observers are usually utilized to augment or replace sensors in control systems in order to avoid non-feasible measurements or to decrease cost. An observer of this kind would have a number of benefits such as increased robustness and stability [37].

1.3 Problem Formulation

After introducing the basic idea and motivation of the work previously, the tasks of this work are described in the following.

The problem formulation for this project is how to investigate and review a model for three-phase LCL filter with nonlinear characteristics of the components and design an observer that calculate continually the voltage over capacitance (U_c) and the current trough L_2 .

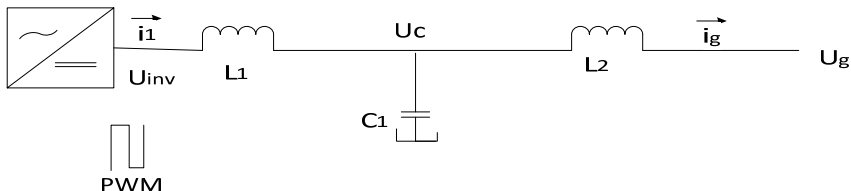


Fig. 1.3 Single-phase LCL filter

The primary goals are to:

- Calculate a model for the three-phase LCL Filter considering with the non-ideal components and make a state-space of the model.
- Use this model and together with the measurement make an observer and a KF that calculates U_c and i_2

Since there are good control tools in Matlab/Simulink and the ADF current control design has been simulated in Matlab as well, it would be the obvious choice for simulating the model and the eventual observer.

1.4 Outline of the Project

This report is divided into 8 main chapters which also represent how the thesis work was done in chronological order.

Chapter 2 gives a short introduction to different line-filter models. This chapter also provides some background on active filters and how they are used to counter power quality issues [35]

Chapter 3 begins with an overview of the three-phase grid connected voltage source converter with LCL filter. Next, a mathematical model for each part of the system is described.

Chapter 4 begins with a short introduction about inductances and their characteristics, and then a model for a nonlinear inductor is developed.

Chapter 5 shows the simulation model and results for nonlinear inductors.

Chapter 6 begins with a definition of the observer and KF, and then proceeds with the mathematical algorithm of a KF in both continuous and discrete time. Finally it describes the observer scheduling method that is used to overcome the nonlinearity.

Chapter 7 presents the simulation results for the linear line filter and nonlinear system with linear observers and the results are analyzed.

Chapter 8 shows a list of references that is used in this work

Two appendices are added to the work, Appendix A is provided the simulations block and how they connected. Appendix B is provided the Matlab codes for KF and the observer used in this study.

2. Line Filters Topology

This chapter describes the line-filters topology and includes a short overview about different sorts of line filters and their constraints.

2.1 Line Filter

In this chapter an introduction to line-filters is described briefly. There are at least three types of line filters but two types of line filters are mostly used in an application of grid-connected voltage source converters: the traditional L-filter and the LCL filter. A lot has been published about line filters and their characteristics [1, 5, 38, and 39]. These filters are used to attenuate common mode noises and normal mode noises generated in electrical devices including a switching power supply source [1]. The frequency of a power switch commonly is about 2-15 kHz, so the voltage source converter will cause high frequency harmonics around the switching frequency. The traditional way to solve the problem is to use an inductor in series with a converter in each phase, the L-filter. This solution works well in low-power systems. However, an unstable system operation and poor system dynamics will accrue for high-voltage power system [38]. In high-voltage power systems the inductance L should be increased to obtain sufficient attenuation of the harmonics that injected by the converter. To decrease the inductance L without affecting the filter, a LCL filter was suggested in 1995 [27]. The LCL filter is a third-order system which is obtained by connecting capacitors, one in each phase, in Y or delta connection on the line side of the L-filter [38]. Furthermore the inductors, one per phase, are connected to the line side of the capacitors. The functions of these inductors are first to stop current harmonics from parallel loads from overloading the capacitors of the line filter and secondly to tune the resonance frequency of the line filter [5]. The LCL filter is even useful when the converter is used to generate reactive power. In this case the capacitors will produce reactive power. Furthermore, the impedance at the grid

side will suffer less stress and lower ripple current stress across the grid inductor [39].

Compared to the L filter the LCL filter is more complex to implement in the control computer but it has better attenuation of the harmonics that are caused by the converter, especially for higher frequencies than the resonance frequency. The other interesting advantage of LCL filters is that they make it possible to lower the value of inductors [5]. Small inductance will improve the response time and stability but a large inductance leads to better filter effect. The choice of the inductance is limited and it is difficult to fulfill all restrictions.

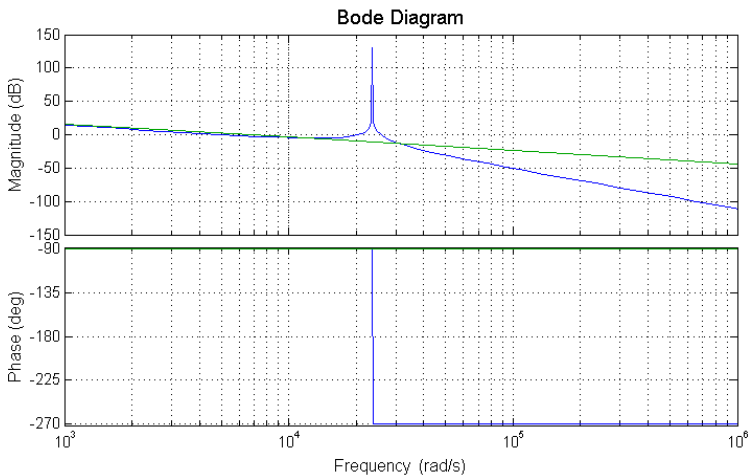


Fig. 2.1 The frequency response (magnitude (top) and phase (bottom)) for undamped LCL filter (blue curve) and Bode plot for undamped L-filter (green curve).

As one can see the LCL filter has good performance in current ripple attenuation even for small inductances. However there is a drawback. The LCL filter brings an undesired resonance effect that generates stability problems. This problem has been solved in an ADF by using the damping resistor in series with the capacitances in each phase, this method is called “passive damping” in literature. There is another better method to damp the resonance peak but this is the task for another thesis.

3. Mathematical Model and Transfer functions for LCL Filters

This chapter starts with an overview of the three-phase voltage source converter connected to the LCL filter. Next, mathematical modeling of the LCL filter and the main circuit of three phase voltage source PWM converter with LCL filters are presented. The model contains the parasitic resistors.

3.1 Background

The three-phase PWM converter with either an inductor as an output filter or more complex output has good functions such as “DC link voltage control [8], sinusoidal input current, unity power factor control and bidirectional power flow”.

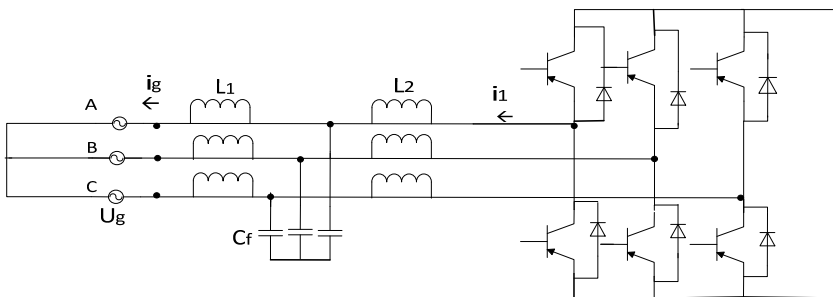


Fig. 3.1 Topology of three-phase voltage source connected with LCL filter on the right side and it connected to the grid on the left side

3.2 Mathematical Model Including Stray Resistor

The choice of component values has a direct effect on grid current i_2 , the converter current i_1 the capacitor current i_c and the capacitor voltage U_c . Transfer functions for the system should be calculated.

To calculate the transfer functions for the system in Fig. 3.1, a single line diagram for the system is drawn as in Fig. 3.2. The components of the filter are considered to be ideal.

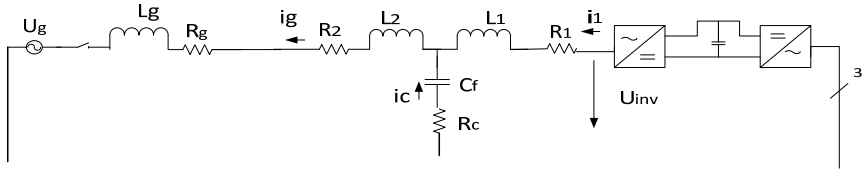


Fig. 3.2 Line diagram for the system

The following equations have been used to investigate the transfer functions for the filter.

$$i_1 - i_c - i_g = 0 \quad (3.1)$$

$$U_{inv} - U_c = i_1(sL_1 + R_1) \quad (3.2)$$

$$U_c - U_g = i_g(sL_2 + R_2) \quad (3.3)$$

$$U_c = i_c(1/sC_f + R_c) \quad (3.4)$$

where the following notation is used:

- U_{inv} , inverter voltage
- U_g , grid voltage
- U_c , voltage drop over filter capacitor
- i_1 , inverter current
- i_g , grid current
- i_c , current through the filter capacitor

- L_1 , filter inductance on converter side
- L_2 , filter inductance on grid side
- C_f , filter capacitance
- R_1 , parasitic resistance in series with L_1
- R_2 , parasitic resistance in series with L_2
- R_c , parasitic resistance in series with c_f

The following transfer functions can be calculated from the converter output voltage to these respective states. These transfer functions are required to show the properties of the system. The properties of the different transfer functions can be illustrated by their transient or frequency response [30].

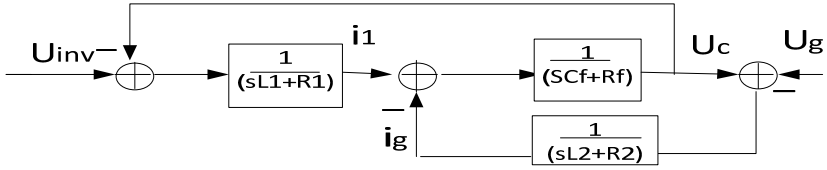


Fig. 3.3 Block diagram for LCL filter with the parasite resistances

The transfer function relating to the voltage at the converter output with the current flowing through the L_2 inductor, $i_2 \rightarrow U_{inv}$, is calculated as Eq. (3.1)

The converter voltage in the Eq. (3.2) should be written as:

$$U_{inv} = i_g(sL_2 + R_2) + (i_c + i_2)(sL_1 + R_1) \quad (3.5)$$

$$U_{inv} = i_g(sL_2 + R_2 + sL_1 + R_1 + \frac{(sL_1 + R_1)(s^2 C_f L_2 + s C_f R_2)}{s C_f R_c + 1}) \quad (3.6)$$

The transfer function for $i_1 \rightarrow U_{inv}$ is calculated as

$$H(s) = \frac{i_1(s)}{U_{inv}(s)} \quad (3.7)$$

$$= \frac{s^2 C_f L_2 + 1 + s R_2 C_f + s R_c C_f}{s^3 C_f L_1 L_2 + s^2 C_f ((L_2 R_c + L_1 R_1) + (L_1 (R_c + R_2))) + s (L_1 + L_2 + C_f (R_c R_2 + R_c R_1 + R_2 R_1)) + R_1 + R_2}$$

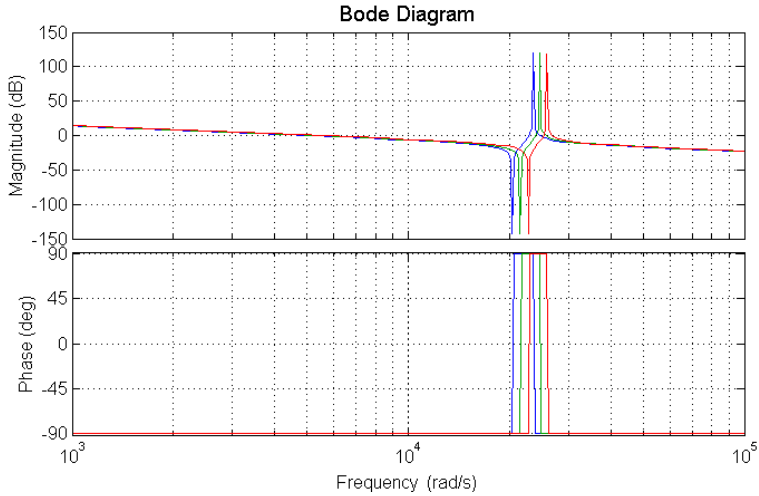


Fig. 3.4 The Bode plot for $i_1 \rightarrow U_{inv}$ when the inductances decrease. ($L_1 = 150 \mu\text{H}$ and $L_2 = 50 \mu\text{H}$ (blue curve)), ($L_1 = 140 \mu\text{H}$ and $L_2 = 45 \mu\text{H}$ (green curve)) and $L_1 = 130$ and $L_2 = 40$ (red curve))

The transfer function from $i_1 \rightarrow U_{inv}$ is used for describing the input-output behavior of the system dynamics and designing the estimator. As one can see in Fig 3.4 the bandwidth of the system is changed by changing the inductances of the inductors.

4. Inductor

This chapter attempts to define the inductor characteristics and then simulate a model of the inductances for the nonlinear inductors.

4.1 Introduction

Inductors are manufactured as coils of conducting material such as copper or aluminum. The core, if any, may be of laminated iron with various alloy additives of iron powder or of ferrite. The physical characteristics of inductors are determined with Eq. (4.1) [2].

$$L = N^2 \mu \frac{A}{l} \quad (4.1)$$

where

- L is inductance in henry [H]
- N is the number of winding turns
- μ is permeability in henry/meter [H/m]
- A is effective magnetic core cross-sectional area in meter [m]
- l is effective magnetic core length in meter [m]

4.2 Inductor Characteristics

Inductors store energy in the form of magnetic fields. Inductance can be defined in several ways. The inductance of a device describes the capability of the device to store the magnetic energy. The energy definition of the inductance is the most fundamental definition of the inductance. But a more popular definition is through the magnetic flux Eq. (4.2).

$$\begin{cases} L = \frac{\Phi}{i} \\ \lambda = \Phi N \end{cases} \quad (4.2)$$

where

- λ flux linkage.
- i is current in Ampère [A].
- Φ is the magnetic flux in weber [Wb].

The magnetic flux is also expressed as

$$\Phi = \frac{N^2 a \mu}{l} \quad (4.3)$$

As can be seen the magnetic flux is proportional to the core permeability. The magnetic flux will change if the permeability of the core is changing.

where

- a is cross-sectional area of the magnetic circuit

The Maxwell and Ampère equations are the set of fundamental laws for time-varying electromagnetic phenomena.

From Faraday's law, voltage is linked to the magnetic flux by Eq. (4.4)

$$V = -\frac{\partial \Phi}{\partial t} \quad (4.4)$$

By substituting Eq. (4.2) into Eq. (4.4) we get Eq. (4.5). It means that the voltage drop across a device is proportional to the time-derivative of the current.

$$V = L \frac{di}{dt} \quad (4.5)$$

In a linear model of an inductor, the permeability is assumed to be constant regardless of the magnitude of the flux in the core. This assumption allows the inductance to remain constant [25]. This simplification is not possible when modeling the nonlinear characteristic, since the core of the inductor will exhibit different material properties.

4.3 Modeling Nonlinear Inductors

Definition

Inductors are generally idealized as obeying the mathematical relations that describe the inductors characteristic [2]. In modeling an ideal inductance, the stray resistance, due to the resistance of the wires, and parasitic capacitance are omitted. However the behavior of the real inductors departs from the ideal, simple inductors. The inductors have nonlinear behavior. The inductors with nonlinear core (the permeability is not constant) have nonlinear behavior. A core may be non-ideal due to its magnetic properties and dimension [26]. The inductance will decrease from its nominal value when the core is saturated. The core will be saturated if the large current goes through the inductor, in which the flux linkage is no longer a linear function of the current.

Magnetic Field Fundamentals

The current that flows into the inductor is a nonlinear function of the flux linkage (λ) and the flux in turn is a function of voltage appearing across the inductors terminals. These relationships between voltage, flux and current are given by Eqs. (4.6-9) for both linear and nonlinear inductances [26].

Linear representation:

$$L = \mu_r \mu_o AN^2 / l \quad (4.6)$$

$$\phi = \frac{iL}{N} \quad (4.7)$$

Nonlinear representation:

$$i = \frac{H_{nonlin} l}{N} \quad (4.8)$$

$$\phi_{nonlin} = B_{nonlin} A \quad (4.9)$$

where

- H is magnetic field strength measured in [A/m]
- B is the magnetic flux density measured in Tesla [T]
- μ_r is relative permeability of core measured in [H/m] = $4\pi \cdot 10^{-7}$
- μ_o is permeability of free space measured in [H/m]

i , H , B and ϕ are non-linear values in nonlinear representation. The non-linearity is defined as an interval around the saturation point in Figs. 4.2-3.

Another common way to represent the magnetic permeability (μ) in the inductor is by representing the relationship between magnetic flux density (B) and magnetic field strength (H).

In linear representation both μ_r and μ_o are constant regardless of the magnitude of the flux in the core. The linear representation is described by Eq. (4.1)

$$B = \mu_r \mu_o H \quad (4.10)$$

In Nonlinear representation the flux density is a function of the magnetic field strength. At each instance of time the core's flux density has different values.

$$B_{nonlin} = \mu_o f(H_{nonlin}) \quad (4.11)$$

The behavior of a saturable magnetic core is typically described in terms of its magnetic flux density vs. magnetic field intensity. There are several possible ways to govern the smooth and effective magnetization B-H curve for inductors with ferromagnetic core material. Some of these methods are published in [24]. One way to create the improved nonlinear B-H curve is by using a Fourier series, based on a set of measurement data [24]. The magnetic energy density can be calculated by the Fourier series expression and then the result is used to terminate the permeability everywhere within the ferromagnetic core. A more thorough description of these methods is outside the scope of the project. But there is another method to get the smooth B-H curve. One approach is based on a determination of analytic expressions of the non-linear inductance. The mathematical expression that I used to plot the BH-curve is represented in Eq. (4.12) [26] and the result is shown in Figs. 4.2-3.

$$B = B_{sat} \tanh(aH) \quad (4.12)$$

where

- B_{sat} is core fully saturated
- a is a coefficient

The magnetic flux-current characteristics of nonlinear inductors and the magnetic field strength-magnetic flux density are plotted in Fig. 4.2 by using the Eqs. (4.6-12) for $L=150\mu\text{H}$ as a test inductance. In these plots the slope of the curve are representing the inductance. The inductance will decrease as current through the inductors increase.

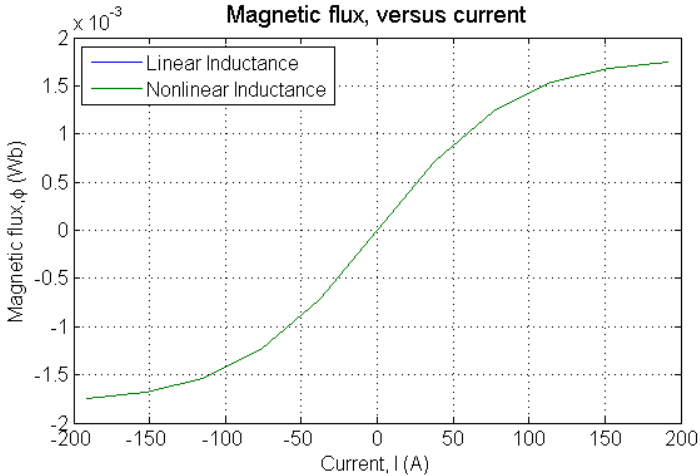


Fig. 4.2 The Magnetic Flux-current curve for $L_1=150\mu\text{H}$ in nonlinear case (green) and for linear case (blue)

Nonlinear Inductance Design

The behavior of linear and nonlinear circuits can be modeled in time-domain using differential equations which usually have the form of differential algebraic equations. For modeling the nonlinear inductances the mathematical constitutive differential Eqs. (4.13-15) are used. The current through the inductor creates a flux, inducing a voltage across the inductor. It means that any change in the current will result in the flux changing. The voltage that is induced by changes in magnetic flux is described by Faraday's law of induction in Eqs. (4.4-5).

$$\frac{d\phi}{dt} = u - Ri \quad (4.13)$$

$$\phi = L(i)i \quad (4.14)$$

$$u = Ri + L(i) \frac{di}{dt} \quad (4.15)$$

where

- R is stray resistance
- $L(i)$, inductance that is depended on current

By taking the integral of the Eq. (4.13) (the voltage across the inductance) the linkage-flux will be calculated. The simulation model for the nonlinear inductance is showed in “simulation tools” chapter 5.

5. Simulation Results

In this chapter the inductance modeling in Simulink environmental is described and the result for the nonlinear behavior of the inductors is shown.

5.1 Simulation Model for Linear LCL Filter

The focus is only on the line filter and the nonlinearity character of the filter components in this part of thesis. The simulation model is developed in MATLAB/Simulink for the purpose of simulating the Line filter in the ADF. This model simulates the electrical three-phase grid, Line-filter and the voltage source converter (Fig. 5.1). The Simulink model is developed so that both linear and nonlinear cases can be studied easily.

5.2 Modeling the Nonlinear Inductance under Matlab/Simulink

In this thesis the focus is on improving the model for the existing LCL filter in an ADF. The work environment has been MATLAB. I used the existing equivalent Simulink circuit for both the converter side of the line filter and the grid side for an ADF to execute and test the new, improved and nonlinear line-filter model. An equivalent circuit of an ADF converter connected to the line-filter is shown in Fig. 5.1, it has six inductors, two for each phase. The components values for the system are shown in Table 5.1.

Table 5.1 lists the system parameters in an ADF.

Symbol	Quantity	Value
R_1	Converter side filter resistance	0.01Ω
R_2	Converter side filter resistance	0.01Ω
R_c	Dampening resistance	0.2Ω
L_1	Converter side filter inductance	$150 \mu\text{H}$
L_2	Converter side filter inductance	$50 \mu\text{H}$
C	Filter capacitance	$0.000016.3\text{F}$
u_{DC}	DC-link voltage	400V

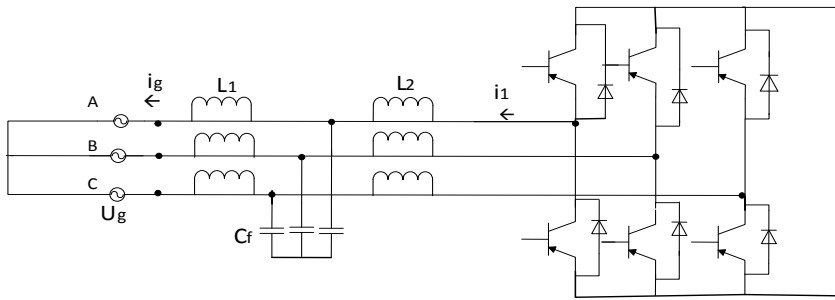


Fig. 5.1 Equivalent circuits of converter, line filter and the grid.

In this thesis the focus is on improving the model for the existing LCL filter in an ADF. The work environment has been MATLAB. I used the existing equivalent Simulink circuit for both the converter side of the line filter and the grid side for an ADF to execute and test the new, improved and nonlinear line-filter. An equivalent circuit of an ADF converter connected to the line filter is shown in Fig. 5.1, it has six inductors, two for each phase. The components values for the system are shown in Table 1.

There isn't any analytical expression representation for the inductors nonlinear characteristics (i.e. shape of the current-flux curve) for the high values of the magnetic flux ϕ . Therefore, I read the data points into the Lookup Table block in Simulink, with ϕ shown on y-axis and i on the x-axis, [26] and then used the linear interpolation between two consecutive points in the iterations on the code under Simulink. The value for ϕ is deduced from the datasheet of the inductors. In other words, this approach can now solve problems with modeling, simulation and optimization of the line filter in the ADF.

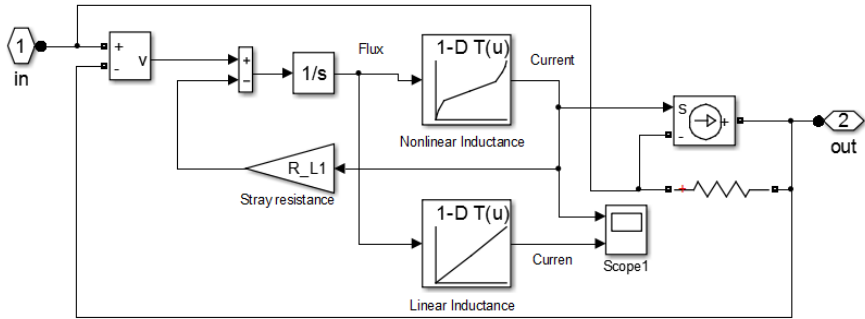


Fig. 5.2 Implementation of the nonlinear inductance under Simulink for $L=50\mu\text{H}$ when L is linear (linear inductance block on top) and when it is not (saturated inductance block at the bottom)

The linear and nonlinear simulation circuits are built by using MATLAB/Simulink, in order to show the differences in current behaviors. These currents will then be used in the estimator design for the LCL filter. By running the model that is shown in Fig. 5.3, the linear and nonlinear cases of the inductance are plotted at the same time. The L_1 and L_2 blocks in Fig. 5.3 are implemented as the Simulink model that is showed in Fig. 5.2. Figure 5.4 shows the inductance behavior of both ideal and real inductors in the model.

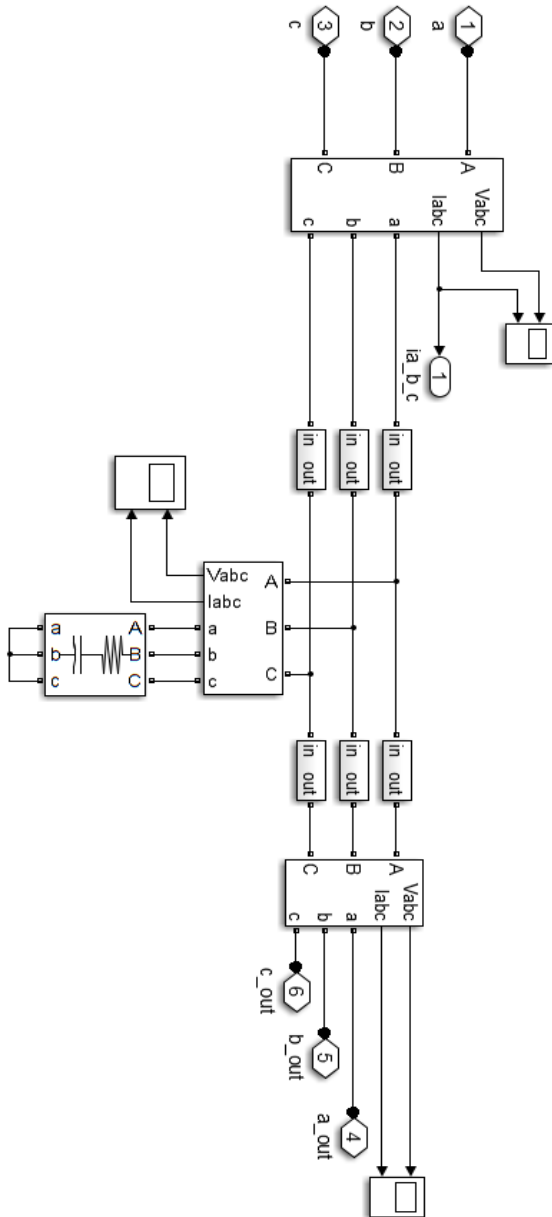
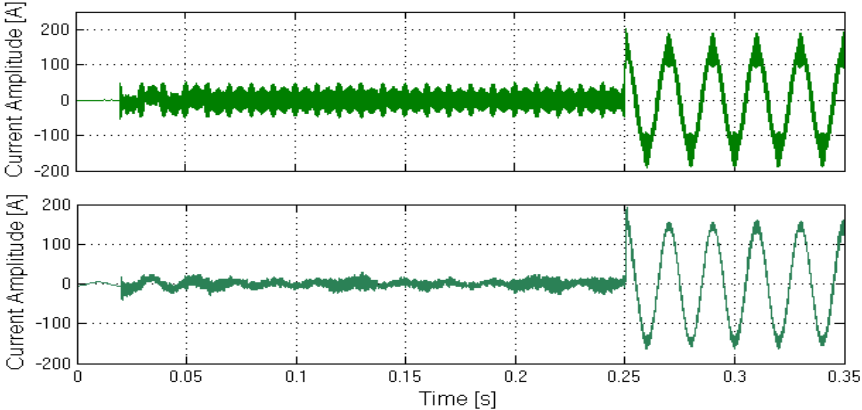
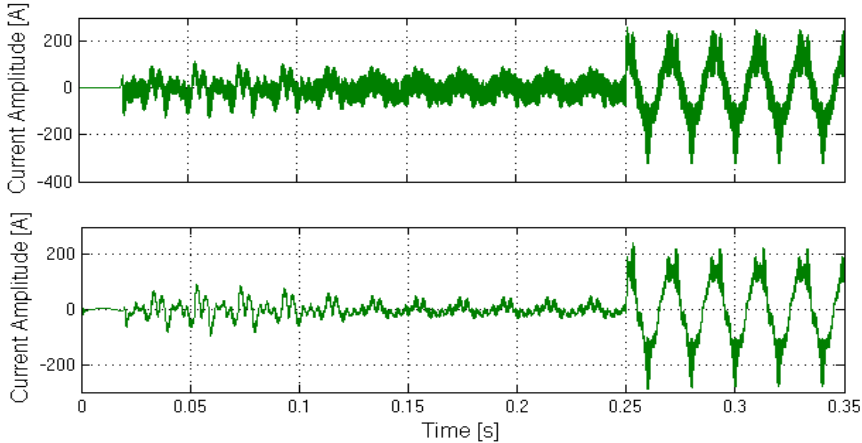


Fig. 5.3 Simulink model of the nonlinear system

The result for the outputs of the nonlinear LCL filter is shown in Fig. 5.5. The converter connected inductance ($L_1= 150 \mu\text{H}$) will be reduced by 20% and the grid connected inductance ($L_2= 50 \mu\text{H}$) will reduce its value by 20% when the converter current goes from 0 A to 200 A.



(a)



(b)

Fig. 5.4(a): The currents shape for linear system (b): the currents shape for nonlinear system. (For (a) and (b) the following is shown from top to bottom: converter current, grid current).

As it is seen in the Fig. 5.4 the nonlinearity is not only changing the shape of the currents but also changes the ripple amplitude. That is because there is always a ripple current through the output inductors as a result of charging and discharging the inductors. This charging and the discharging are caused by the transistor switching. As one can see the ripple current becomes higher when the inductors are nonlinear.

The effect of the nonlinearity is visible in the wave form of the current, which is highly distorted.

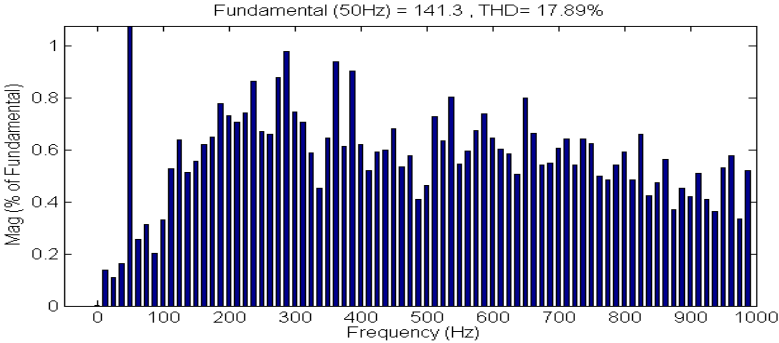


Fig. 5.5 The FFT (fast Fourier Transformer) diagram of the converter current when the linear inductors are applied to the system

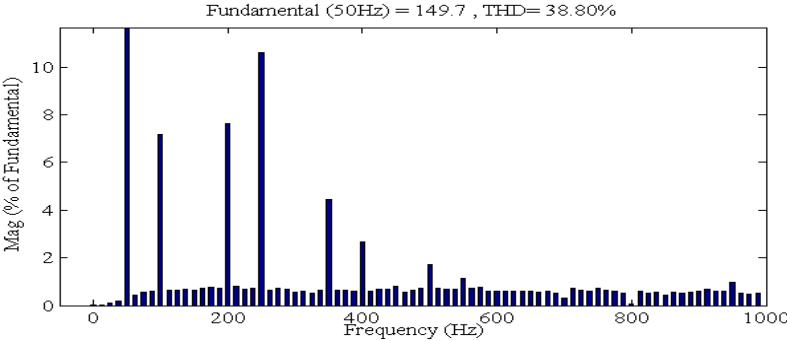


Fig. 5.6 The FFT diagram of the converter current when the nonlinear inductors are applied to the system

Analysis of the Influence of Inductor Saturation

As can be seen in the Fig. 5.4 the difference between the current waveform's results for the models are great. These two curves (Fig. 5.4) are fitted only in the linear area. The elimination of the nonlinearity of the components in the LCL filter model will lead to failure of the model. In Fig. 5.4 one can compare the currents shape and magnitude through the L_1 and the L_2 in the LCL filter for both linear model inductance and nonlinear model inductance. The inverter output current, the grid input current and the capacitance current are shown for both linear inductors and the nonlinear ones under the same circumstances. By comparing the converter current that is showed in both Fig 5.4 and Fig. 5.5 one can see how the nonlinearity of the inductors affect the shape of the current, i.e. in Fig 5.4 the inductance reduces its value by more than 20% when the amplitude of the current increases. In Figs. 5.5-6 the converter current ripple is plotted in the frequency domain.

Conclusion and Future Works

The purpose of the first part of my thesis has been to compare the features and the capabilities of available inductor models and a possible way to implement advanced, correct saturated behavior of the inductors in an ADF. In order to overcome limitations due to the limited amount of information about flux saturated values estimated values of flux density has been used for both L_1 and L_2 in the line filter.

The outcome of this part of the investigation suggests that the ADF lacks an advanced, nonlinear inductance model. The nonlinear inductance has been simulated and it showed good potential, but more work has to be done to refine the estimation of the magnetic flux and magnetic strength field from available data for each inductor in the ADF. Thus, an improved procedure for modeling the nonlinear characteristic of the inductors with ferromagnetic material, in this case SF16, is needed at present.

6. Observer Algorithm and Parameters

This chapter covers the state-space form of the line filter representation and related Kalman filter theory. The scheduled observer theory is presented at the end.

6.1 Theoretical Formulation of the Kalman Filter

The original Kalman filter (KF) presented by R. E. Kalman in 1960 was designed for linear models. The KF is one of the most well-known and optimal linear estimators based on an iterative process (least-squares error) which means the new measurements can be processed as they arrived [41]. The KF produces an optimal estimate of the state in the sense that the mean value of the sum (any linear combination) of the estimation error gets a minimal value [14]. Another benefit of the KF is that it is recursive in discrete time, which allows reprocessing without storage of previous data. It recursively evaluates an optimal estimate of the state variable. At each iteration a new estimate of the state will be evaluated. This estimated state is based on the previous state estimate, which allows efficient real-time calculation [13]. The new information is now available to the filter and can be used. In our case, the state parameters are the voltage over the line filter capacitance and the current through the net. The KF is not optimal to use for non-linear systems and non-Gaussian filters [11]. One early attempt to adapt KF to nonlinear problems was done by using the Extended Kalman Filter (EKF). EKF uses the original KF, [10] [12] [14], EKF simply linearizes the non-linear model so that the KF can be applied to it.

There are two well-known drawbacks of using the EKF:

1. The derivation of the Jacobian matrices [42] is nontrivial and lead to implementation difficulties
2. Calculation of Jacobian matrices can be very difficult [15]; making the implementation of EKF hard to achieve.

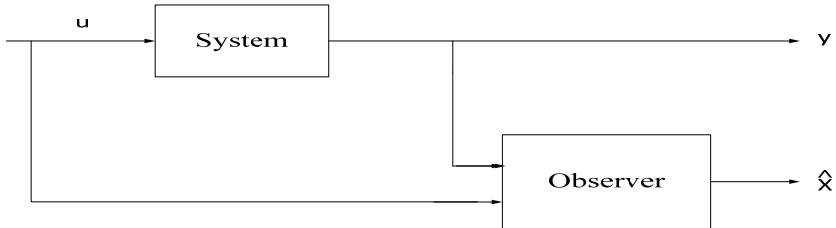


Fig. 6.1 Shows the inputs and the output of an observer

EKFs may not perform well enough in cases of large scale nonlinear problems or highly nonlinear dynamics [10] but EKFs are widely used in applications.

6.2 General Information

State-space Form

A state-space representation is a mathematical model of a, dynamic system as a set of inputs, outputs and state variables related by a set of first-order differential equations.

Most signal input and output relations can be described by a differential equation, and the state-space representation may provide a compact and convenient way to model and analyze the system.

State Vector

The state vector contains the variables which should be predicted. Often variables in the state vector cannot be measured directly or it is not economical to do so, these variables must be inferred from the measured variables.

If the full state vector is not available to measurement it can be reconstructed from available measurement signals and an input signal from a model. This can be done in several ways.

Reconstruction through direct calculations: this method is the most straight forward approach to reconstruct the states by using the input and output signals. This method has the drawback that it may be sensitive to disturbances [4]. The method takes information from k different sampling instants. This method is not used in this thesis but it is described deeply in [4].

Observer-based reconstruction: this method uses the model information explicitly. This is a better alternative. The method gives the state as a function of past inputs and outputs. The reconstruction can be improved by using the measured outputs. This can be done by introducing a feedback from the difference between the measured and estimated outputs, $y - C\hat{x}$.

The reconstructed signals in this work are obtained by using the second method, Observer-based reconstruction.

6.3 Kalman Observer Design for LCL Filter

In Chapter 3 the mathematical model of the system and its transfer functions are briefly described. The differential equations of the system are derived in Eqs. (3.1-4). The state-space form of the system is derived by using these equations and by knowing the state variables and the measured signals for the system.

Continuous-Time State-Space System

Analytical system modeling can be performed in the discrete or continues time plane. In this work first continuous time modeling will be described and then, discrete modeling will be used.

$$\frac{d}{dt} \underbrace{\begin{pmatrix} i_1 \\ U_c \\ i_g \end{pmatrix}}_x = \underbrace{\begin{pmatrix} -\frac{R_1+R_c}{L_1} & -\frac{1}{L_1} & \frac{R_c}{L_1} \\ \frac{1}{C} & 0 & -\frac{1}{C} \\ \frac{R_c}{L_2} & \frac{1}{L_2} & -\frac{R_2+R_c}{L_2} \end{pmatrix}}_A \begin{pmatrix} i_1 \\ U_c \\ i_g \end{pmatrix} + \underbrace{\begin{pmatrix} \frac{1}{L_1} \\ 0 \\ 0 \end{pmatrix}}_{B_1} U_{inv} + \underbrace{\begin{pmatrix} 0 \\ 0 \\ \frac{-1}{L_2} \end{pmatrix}}_{B_2} U_g \quad (6.1)$$

$$y = \underbrace{(1 \ 0 \ 0)}_C \begin{pmatrix} i_1 \\ U_c \\ i_g \end{pmatrix} \quad (6.2)$$

An explicit continuous-time state-space technique is used and it given by Eqs. (6.1-2). In this case the output of the LCL filter is the measured variable, the

filter current (i_1), which is the same as the inverter current and A , B_1 , B_2 , and C are the continuous time state-space matrices that express the system dynamics. Where the state variables are converter current, i_1 , the capacitor voltage, u_c , and the grid current, i_g . The measured inputs to the system are u_{inv} , the voltage applied by converter and grid voltage, u_g . The output is the converter current, i_1 . The deterministic part of the model is described in the A matrix and describes how the estimate propagate with the time. Rewriting Eqs. (6.1-2) in compact form, one has

$$\begin{cases} \dot{x}(t) = Ax(t) + B_1U_{inv}(t) + B_2U_g(t) + v_1(t) & (\text{state equation}) \\ y(t) = Cx(t) + v_2(t) & (\text{measurement equation}) \end{cases} \quad (6.3)$$

where

- v_1 is an additive process noise term with covariance Q
- v_2 is an additive measurement noise with covariance R which is uncorrelated with v_1

The use of a state estimator lets us obtain the complete state vector from the measurement of the converter voltage and current and grid voltage. Here we need the dynamic of the estimator. An observer is an open loop model of the system which includes a correcting term based on the measured output [28].

$$\begin{cases} \dot{\hat{x}}(t) = A\hat{x}(t) + Bu(t) + K(y - \hat{y}) \\ y(t) = C\hat{x}(t) \end{cases} \quad (6.4)$$

The continuous-model (6.3) is given and the problem is to estimate the states from observation of y and u . The quality of the estimate $\hat{x}(t)$ can be assessed by the quantity $y(t) - C\hat{x}(t)$. If $\hat{x}(t)$ is equal to $x(t)$ and there is no measurement noise, the quantity would be zero. By feeding back this measurement of the quality of $\hat{x}(t)$ to the simulation we obtain the observer (6.5).

$$\dot{\hat{x}} = A\hat{x} + B_1U_{inv} + B_2U_g + K(y - \hat{y}) \quad (6.5)$$

$$\hat{y} = C\hat{x} \quad (6.6)$$

where

- \hat{x} is an observer state vector and the diacritic (^) denotes that it is an estimated quantity
- \hat{y} is the observer output signals
- K is the KF gain

Since the goal here is that $\hat{x}(t)$ should be close to the true state $x(t)$, the estimate error is defined as:

$$\tilde{x}(t) = x(t) - \hat{x}(t) \quad (6.7)$$

By substituting the Eqs. (6.3) and (6.5) we will get:

$$\dot{\tilde{x}}(t) = (A - KC)\tilde{x} + v_1 - Kv_2 \quad (6.8)$$

From the above equation, it is seen that the Kalman gain, K , affects the estimation error both on the determining the matrix $(A - KC)$ and measurement error, Kv_2 . The KF's features would be decided by eigenvalues of the matrices $(A - KC)$ and therefore the choice of vector K is a balance between sensitivity to the measurement disturbances and adaptability to the influence of the system disturbances [30]. This determines how fast we need to reconstruct the states (eigenvalues $(A - KC)$) and how sensitive we can be to the measurement disturbances (Kv_2) [30]. A fast observer will converge quickly, but it will also be sensitive to measurement error v_2 .

There are various different ways to determine the matrix K . To determine K we introduce the reconstruction error (6.7). The matrix K should be selected so that the state estimation error goes to zero asymptotically. By introducing a feedback from the measurements in the reconstruction, it is thus possible to make the error go to zero. In other words the K matrix should be chosen so that the matrix $(A - KC)$ has prescribed eigenvalues. However, this problem is solved in connection with the pole-placement problem. In this work the poles for the observer are placed 3 times faster than for the dynamic system and the Matlab commands *eig(A)*, *acker* and *kalman* are used in order to place the observers poles in the desired place. As I mentioned before the selection of the observer poles is a trade-off between sensitivity to measurement errors and rapid recovery of initial error [4]. A fast observer will converge quickly, but it will also be sensitive to measurement errors.

Another way to determine the optimal filter gain K with considering both the process disturbances and the measurement noises is by solving an algebraic Riccati equation [30]. See Eqs. (6.9-11)

$$K = PC^T R_2^{-1} \quad (6.9)$$

where

- R_2 is the noise covariance matrix
- P is the symmetric positive semi definite matrix

P is also equal to the prediction error covariance matrix of the optimal estimation error, the solution to the Algebraic Riccati equation. The goal is to find the minimum of this matrix. This occurs by Eq. (6.12).

$$\lim_{t \rightarrow \infty} P = \lim_{t \rightarrow \infty} E\{[x(t) - \tilde{x}(t)][x(t) - x(t)]^T\} \quad (6.10)$$

$$AP + PA^T - (PC^T + NR_{12})R_2^{-1}(PC^T + NR_2)^T + NR_1N^T = \dot{P} \quad (6.11)$$

If the linear model is time invariant then a steady-state version of the system can be found. This is done by setting \dot{P} in Eq. (6.11) to zero. In this case the state, input, output, Kalman gain and covariance matrices become time invariant.

The state error covariance matrix is a square and symmetric matrix (6.10), and must remain positive definite in order for filter stability to be retained [31]. Diagonal elements of this matrix are variances of errors of the estimations for corresponding components of the state vector.

The solution of the Riccati equation was found to provide a measure of how well the state variables can be estimated in terms of mean-square estimation error. These nonlinear matrix Riccati equations are particularly significant in optimal control, filtering and estimation problems. Riccati equations play significant roles in optimal control of multivariable estimation.

The covariance matrices, Q and R are determined as part of a system identification procedure [36]. For an initial guess of the covariance value, a very large value could be selected if very poor sensors are used for the measurements. This makes the filter very conservative. The opposite will happen if very good sensors are used for measurement [31].

The optimal gain matrices K in Matlab is given by state-space model, SYS, of the plant and covariance matrices Q and R (see below).

$$[\text{Observer}, k] = \text{Kalman}(\text{SYS}, Q, R) \quad (\text{Matlab command})$$

The Q and R parameters are design parameters with the origin in process noise and the measurement disturbance in (6.1).

The matrices Q and R can be calculated from measurement data by means of system identification [36].

Discrete Time

Micro-controller measurements are described with discrete equations and since the KF will be implemented on a micro controller the discrete KF form will be used. Time is given in discrete interval and denoted with subscript k .

The treatment of measurements is completely identical with the continuous time in the discrete time case. The observer formulation in the discrete time domain has the advantages of the straight forward modeling when additional time delays are considered. By taking the characteristic zero-order hold behavior of the analog-to-digital signal conversion into account, the equivalent state space model in the discrete time domain is derived using the transformation laws presented in [29] (6.12-13).

$$A_d = e^{AT_s} \quad (6.12)$$

$$B_d = \int_0^{T_s} e^{At} B dt \quad (6.13)$$

where

- A_d is the discretized matrices of A
- B_d is the discretized matrices of the B with sampling time T_s

The resulting state-space model for the LCL filter is presented by using the Matlab command `c2d` with 14 kHz sampling frequency.

The measurement is unchanged but discrete.

$$\frac{d}{dt} \begin{pmatrix} i_1(k+1) \\ U_c(k+1) \\ i_g(k+1) \end{pmatrix} = \begin{pmatrix} a_{11} & a_{12} & a_{13} \\ a_{21} & a_{22} & a_{23} \\ a_{31} & a_{32} & a_{33} \end{pmatrix} \begin{pmatrix} i_1(k) \\ U_c(k) \\ i_g(k) \end{pmatrix} + \begin{pmatrix} b_{11} & b_{12} \\ b_{21} & b_{22} \\ b_{31} & b_{32} \end{pmatrix} \begin{pmatrix} U_{inv}(k) \\ U_g(k) \end{pmatrix} \quad (6.14)$$

The observer by stationary KF is determined according to state Eq. (6.14).

$$\begin{cases} \hat{x}(k+1) = A_d \hat{x}(k) + B_d u(k) + K(y(k) - \hat{y}(k)) \\ y(k) = C_d \hat{x}(k) \end{cases} \quad (6.15)$$

A discrete- time representation of (6.4), with sampling period T_s is given by (6.16)

$$\hat{x}(k + 1) = (A - KC)\hat{x}(k) + B_1U_{inv}(k) + B_2U_g(k) + K(y(k)) \quad (6.16)$$

State estimation error for the model in discrete time (6.18). Let the error be the difference between the state and the state estimate.

$$e(k) = x(k) - \hat{x}(k) \quad (6.17)$$

Furthermore, the mean value of the state estimation error covariance matrix which will be called P_k is defined as (6.18).

$$P_k = E\{[e(k)e(k)^*]\} \quad (6.18)$$

$$P_{k+1} = Q(k) + [A(k) - KC_d(k)]P(k)A^T(k) \quad (6.19)$$

Based on the a priori estimate and its error covariance, P , the KF gain is computed as Eq. (6.20) [40].

$$K(k) = P(k)C^T(k)[(C(k)P(k)C^T + R)]^{-1} \quad (6.20)$$

The gain matrix is computed, followed by prediction of the state vector at the next time step. As in the case of continuous time if the state representation of the system is linear time invariant, the steady state version of the filter can be used.

The design problem concerns how to choose K so that all eigenvalues of $A - KC$ are within the stability domain (implementation of equations are shown in appendix B)

6.4 Observer Scheduling

The state and parameters estimation problem for nonlinear systems and the classical solution, Extended Kalman Filter (EKF), for such problems have been widely discussed in the literature [17]. In order to overcome some EKF drawbacks, different improvements of this algorithm have been proposed.

The solution proposed in this thesis is called Observer Scheduling. Inspired by the popular theory of gain scheduling, the idea, depicted in Fig. 6.2 using three

observers. Observer scheduling is switching or blending the dynamics matrix (A) values, observers or models depending on the operating conditions. Observer scheduling may either involve continuous or discrete scheduling of the observers with the respective dynamic model. Conceptually, observer scheduling is based on a linear, time-invariant, parameter dependent plant [5]. Three different observers are parallel connected in this work and each filter has its own state vector. In particular each KF has been chosen so that the complete nonlinear estimation problem is divided into three linear time-varying parallel sub-problems. This solution is a simple approach to overcome the complexity of the EKF. A scheme of the observer scheduling idea is showed in Fig. 6.2.

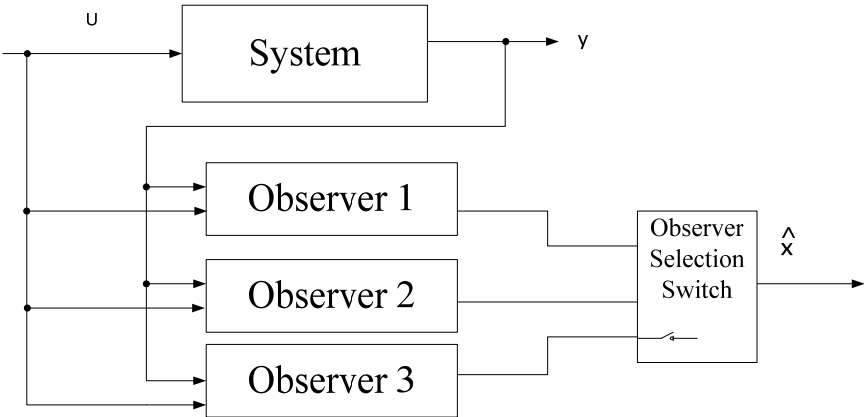


Fig. 6.2 Observer scheduling scheme

6.5 Scheduling Approaches

This thesis evaluated two gain scheduling approaches:

Kalman Filter Scheduling

In this case, three linear parallel KFs are used to create an observer bank, in which each observer is tuned to have a specific operating point. Then a switch block is used to provide the selection of the observer at each sample as a source of the estimated state values. This switching method is based on the measured values of the signal, in this case the converter current. This measured signal must have a strong correlation with the internal states. The scheduling method is simple and

has no stability problems because each KF in the observer bank is linear and constitutes a linear feedback filter, which has no nonlinear terms and model uncertainty, and is therefore stable by construction.

Observer Scheduling

Linearization based on scheduling yields a set of locally valid, linear parameter-dependent plant models.

7. MATLAB/Simulink Result

The objective of this chapter is to present and discuss the results of the simulations of the equations described in Chapter 6 of the line-filter model for an active dynamic filter and the KF. The result is showed for an observer and a KF. Two different sampling frequencies have been run and plotted for each case.

7.1 Experimental setup

To check if the KF has sufficient performance during time-varying operation, the algorithm has been implemented using the KF theory (explained in the previous chapter) using Simulink tools and Matlab-functions (presented in Appendix A).

The KF function reconstructed the capacitance voltage and the grid current signals and returns them into the ADF controller. For all of the result the sampling rate of 14 kHz has been used. The construction has also been tested with higher sampling rate.

The block diagram of the simulated system is shown in Fig. 7.1. The system was built using the Power System Toolbox in Simulink. Fig. 7.2 shows the KF block diagram that was implemented for the controller.

The Simulink model for the observer schedule is shown in Fig. 7.3 and the Matlab embedded function for the KF is attached in appendix B.

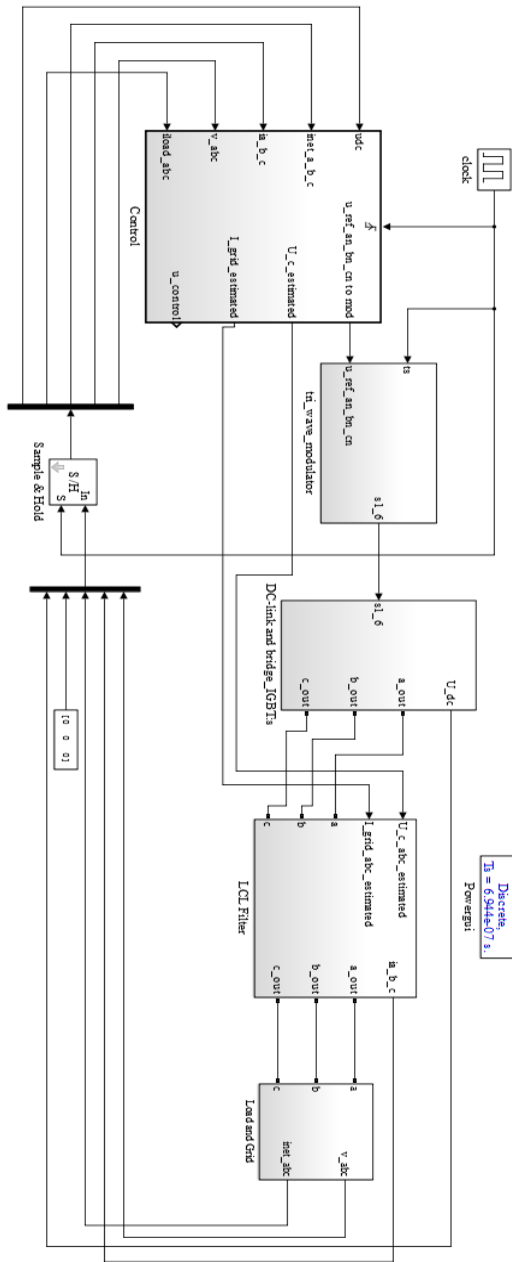


Fig. 7.1 Simulink model of grid connected inverter

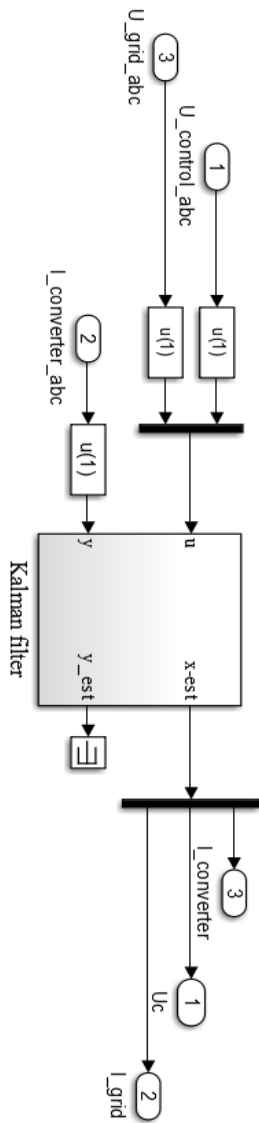


Fig. 7.2 Simulink model of the KF with the inputs signal and the outputs signals

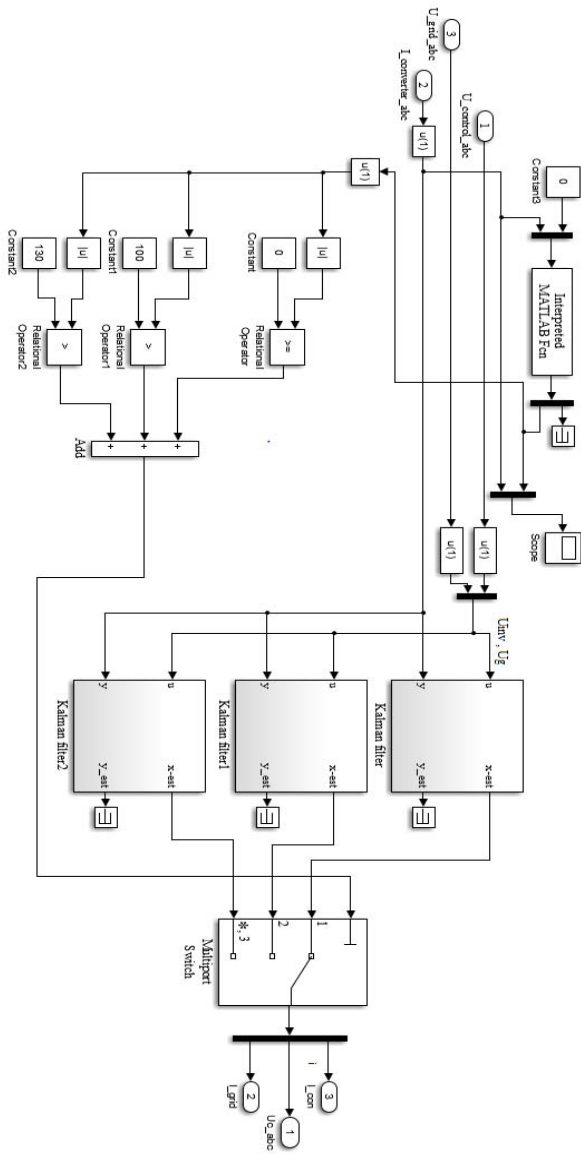


Fig. 7.3 Observer schedules for nonlinear plant

7.2 Simulation for Linear System Dynamics

Linear System Dynamics

An alternative to the KF is an observer, it has the same structure as the KF but it is estimating the signals from specific estimator errors. The algorithm of the observer for the linear LCL filter has been tested in absence of measurement disturbances and process noise using Matlab and the SimPowerSystems Toolbox.

The basic simulation setup consists of a voltage source converter (VSC) of 400 kVa connected to an ideal grid generator by means of an LCL filter similar to the one used in the experimental test.

The measured and the estimated waveform for the states that is described in the previous chapter is simulated and shown in Fig. 7.4. A very good grid current and capacitance voltage performance is achieved. The poles are placed 10 times faster than the system poles and I did it by using Matlab commands that are mentioned in chapter 6. A load will be connected to the system at time 0.25s and it shows up as a step in all Figures. The discrete system model that I have used in this Simulation is:

$$\begin{cases} \hat{x}(k+1) = A\hat{x}(k) + B_1 U_{inv}(k) + B_2 U_g(k) \\ y(k) = C_d \hat{x}(k) \end{cases}$$

where

$$A = \begin{pmatrix} 0.7150 & -0.2797 & 0.2790 \\ 0.8157 & -0.1272 & -0.8099 \\ 0.8679 & 0.8639 & 0.1202 \end{pmatrix}$$

$$B_1 = \begin{pmatrix} 0.4424 \\ 0.2750 \\ 0.1627 \end{pmatrix}$$

$$B_2 = \begin{pmatrix} -0.1627 \\ 0.8522 \\ -1.0266 \end{pmatrix}$$

$$C_d = (1 \ 0 \ 0)$$

The observer that I have used is:

$$\begin{cases} \hat{\dot{x}} = A\hat{x} + B_1u_{inv} + B_2u_g + K(y - \hat{y}) \\ \hat{y} = C\hat{x} \end{cases}$$

when $K = \begin{pmatrix} -0.0601 \\ 1.2169 \\ 0.4016 \end{pmatrix}$ the observers poles will be placed ten times faster.

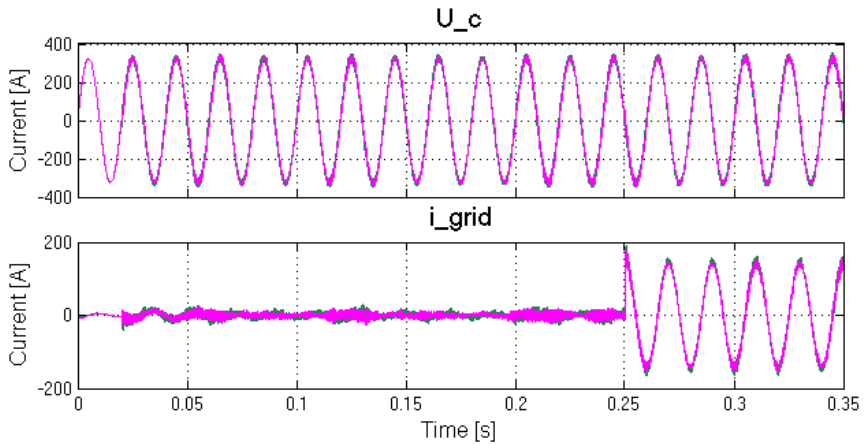


Fig. 7.4 The two plots on top: capacitance voltage (green) and estimated capacitor voltage (pink) in one phase, grid current (green) and estimated grid current (pink) in one phase

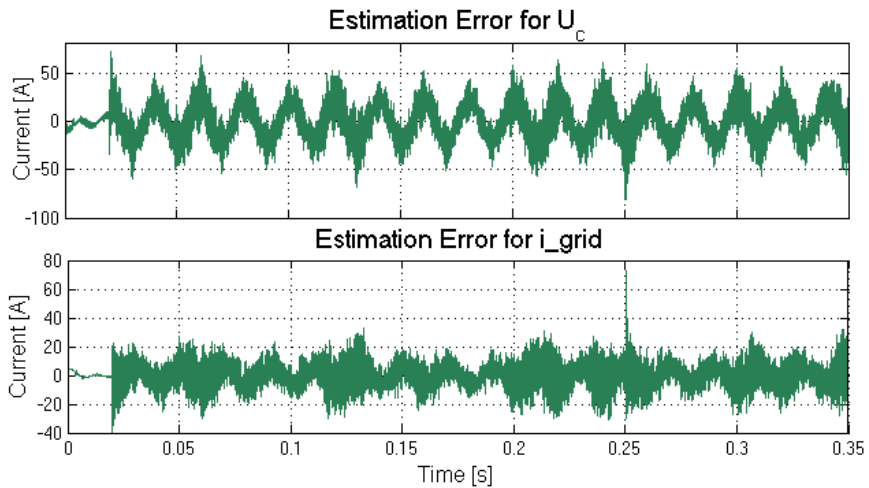


Fig. 7.5 The estimation error for the capacitance voltage (top) and for the grid current (bottom)

In these Figures the observer had a sampling frequency equal to 14 kHz while the signals that should be estimated are 100 times faster sampling frequency. As one can see the estimator is following the analog signal well but it cannot follow the ripples on the signals. In order to follow the signal and even the

ripple for the signal, the sampling frequency must be at least twice the ripple frequency according to Nyquist theorem.

Studying the Effect of Sampling Frequency

The objective of this section is to investigate how sampling frequency affect the choice of the poles and accuracy of estimated signals. Different sampling frequencies were applied to the observer. The result was compared and showed in this section. Two scenarios have been simulated:

- Scenario 1, lower sampling frequency for the observer than for the system
- Scenario 2, The KF was sampled with high frequency.

Scenario 1: Observer with Low Sampling Frequency

In order to test the effect of the sampling frequency on the observer, the observer is updated once every 10 samplings. In Fig. 7.6 the result for an observer with 10 times lower sampling frequency than the measured signal is showed (Code for this experiment is showed in Appendix B). This test was applied in a Matlab script not in the Simulink environment which means that the system as well as the observer is ideal, the sampling frequency was 100 kHz (see Table 7.1). In the Fig. 7.6 the observer has been sampled at a lower frequency than the system. In order to study the effect of the low sampling frequency an error plot for the signals is done, see Fig. 7.7. In order to be able to compare the estimation error for lower sampling frequency with that for higher sampling frequency plots for the estimation error has been done (see Fig. 7.7-8), the system and the observer have the same sampling frequency in Fig. 7.8 and the observer has lower sampling frequency in Fig. 7.7.

Symbol	Quantity	Value
R_1	Converter side filter resistance	0.01 Ω
R_2	Converter side filter resistance	0.01 Ω
R_c	Dampening resistance	0.01 Ω
L_1	Converter side filter inductance	150 μH
L_2	Converter side filter inductance	50 μH
C_f	Filter capacitance	0.00005 F

U_{inv}	DC-link voltage	1 V
f_s	Sampling frequency for observer	10 kHz
f_{sys}	Sampling frequency for system	100 kHz

Table 7.1 the component values that are used in the scenario

The system dynamics that is implemented in this scenario is showed below:

$$A = \begin{pmatrix} -0.0133 & -0.6667 & 0.0067 \\ 2.0000 & 0 & -2.0000 \\ 0.0200 & 2.0000 & -0.0400 \end{pmatrix} 1.0e+04,$$

$$B_1 = \begin{pmatrix} 0.6667 \\ 0 \\ 0 \end{pmatrix},$$

$$B_2 = \begin{pmatrix} 0 \\ 0 \\ -2 \end{pmatrix},$$

$$C_d = (1 \ 0 \ 0),$$

$$K = \begin{pmatrix} -0.1456 \\ 0.1544 \\ 1.3574 \end{pmatrix}$$

Observer poles are placed on $(0.9048 + 0.0000i, -0.3640 - 0.7182i, -0.3640 + 0.7182i)$ while the system poles are placed on $(0.3718, 0, 0) \cdot 1.0e-43$

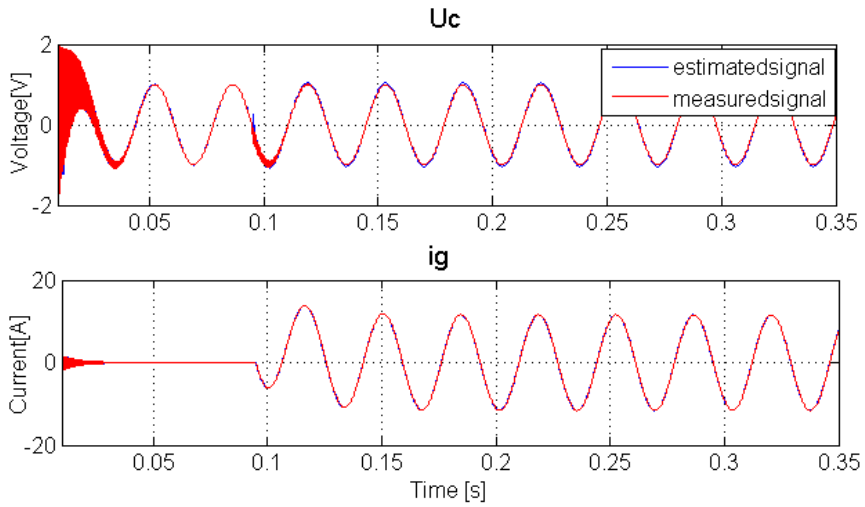


Fig. 7.6 The two plots on top are: capacitance voltage (red) and estimated capacitance voltage (blue), grid current (red) and estimated grid current (blue) when the estimator were sampled 10 times slower than the system were sampled.

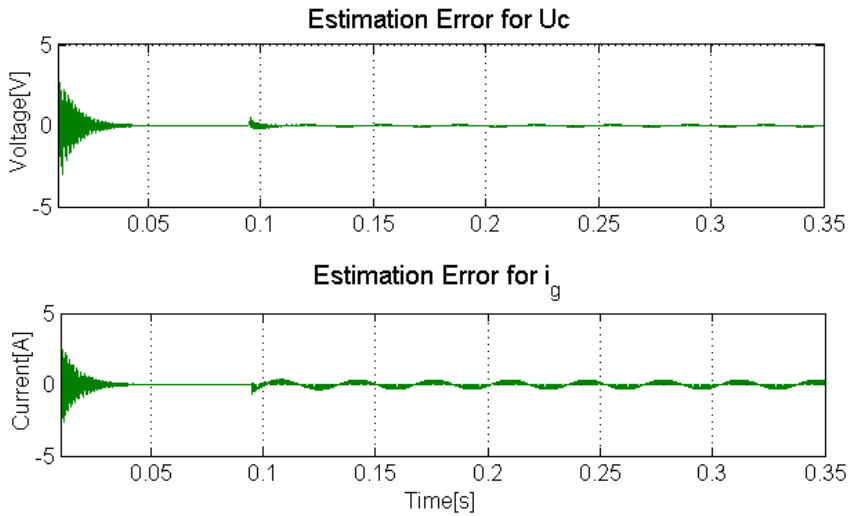


Fig. 7.7 The estimation error for the capacitance voltage (top) and for the grid current (bottom)

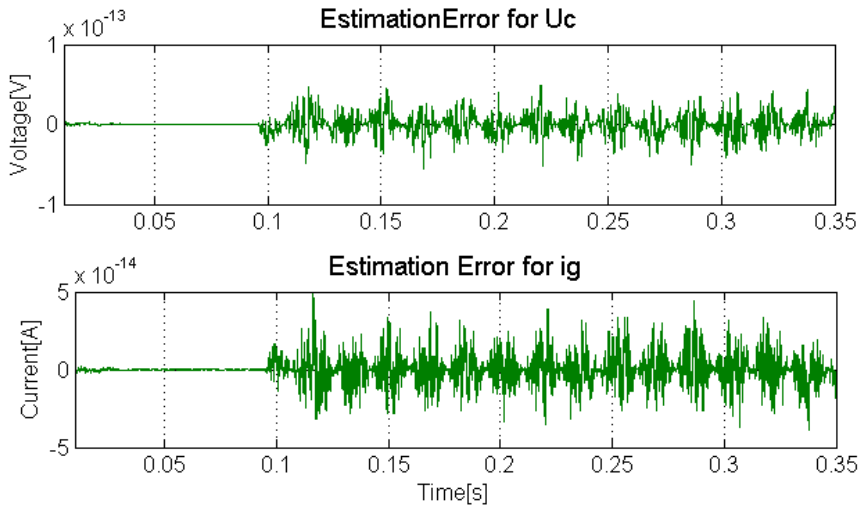


Fig. 7.8 The estimation error for the capacitance voltage (top) and for the grid current (bottom) when the observer has the same sampling frequency as the system

The slow estimator (see Fig. 7.6) has less accuracy than the fast observer. The result is benchmarked by comparing Fig. 7.7 with Fig. 7.8.

Result for this test showed that in order to track the signals with this slow observer (scenario 1), the observer poles needed to be placed faster. The poles should have been placed far from the origin on the negative side of the coordinate system in the continuous time domain in order to correctly reconstruct the signals. The observer will be implemented in the FPGA and this micro controller has sampling frequency 14 kHz and the signal that should be estimated have sampling frequency at least 100 times faster which means that scenario 1 is the actual scenario for the ADF.

Scenario 2, Case 2: The KF Design with High Sampling Frequency

A KF has been designed in Matlab/Simulink for the system with the same parameters as the observer (see the previous subsection) in order to compare the performance of the KF with the observer. The KF with high sample frequency are plotted and shown in Figs. 7.9-12. The Table below shows the specification for the components and the frequencies in this scenario.

Table 7.2 the component values that are used in this scenario

Symbol	Quantity	Value
R_1	Converter side filter resistance	0.01 Ω
R_2	Converter side filter resistance	0.01 Ω
R_c	Dampening resistance	0.2 Ω
L_1	Converter side filter inductance	150 μH
L_2	Converter side filter inductance	50 μH
C_f	Filter capacitance	0.000016.3 F
U_{inv}	DC-link voltage	400 V
f_{FPGA}	FPGA sampling frequency	14 kHz
f_{sys}	Sampling frequency for system	1400 kHz
f_{HS}	High Sampling frequency for observer	140 kHz
f_s	Sampling frequency for observer	14 kHz

For plots in Fig. 7.8 and the discrete system dynamics with sampling frequency equal to 14 kHz and the weighting matrices are described as below:

$$A = \begin{pmatrix} 0.7272 & -0.2767 & 0.2673 \\ 0.8648 & -0.0498 & -0.8596 \\ 0.8018 & 0.8252 & 0.1872 \end{pmatrix},$$

$$B_1 = \begin{pmatrix} 0.4155 \\ 0.2631 \\ 0.1388 \end{pmatrix},$$

$$B_2 = \begin{pmatrix} -0.1389 \\ 0.7866 \\ -0.9640 \end{pmatrix},$$

$$C_d = (1 \ 0 \ 0)$$

Measurement disturbances: $R = 1$

The process disturbance: $Q = \text{diag}([1 \ 0 \ 1])$

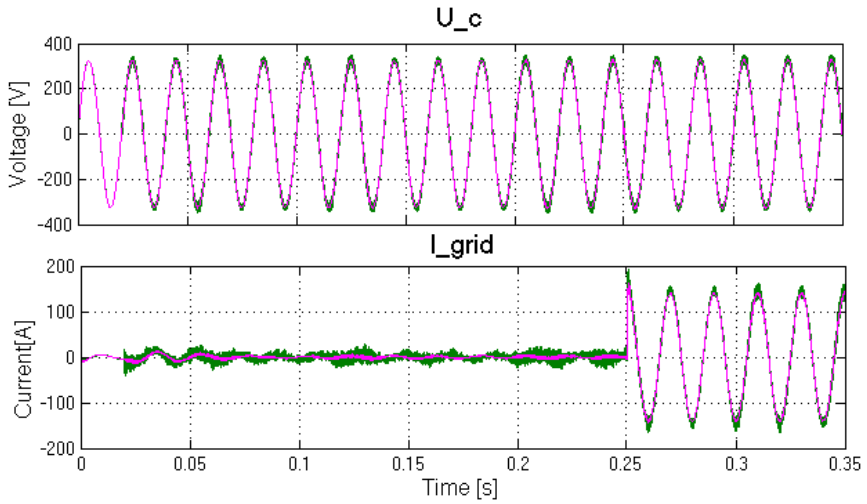


Fig. 7.9 Two plots on top are: capacitance voltage (pink) and estimated capacitance voltage (green), grid current (pink) and estimated grid current (green) for the KF for with sampling frequency =14 kHz

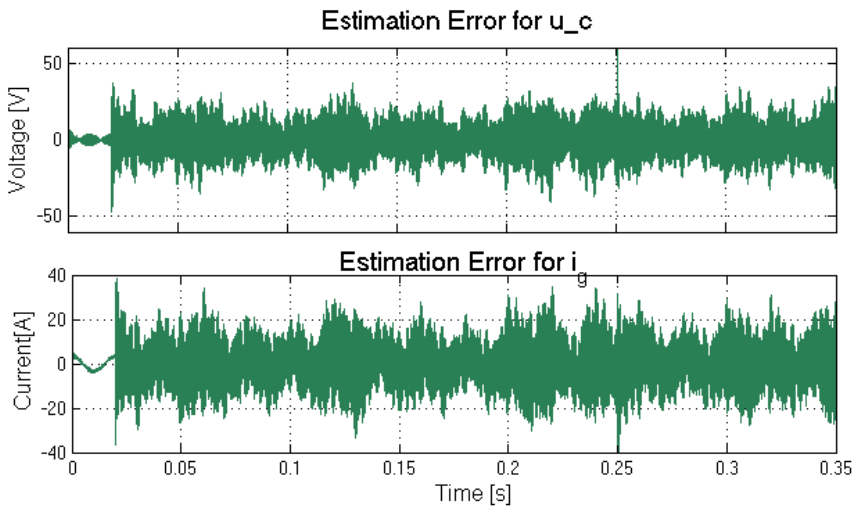


Fig. 7.10 The estimation error for the capacitance voltage (top) and for the grid current (bottom)

An analysis of the estimation error has been done and it is showed in Table 7.3

Table 7.3 the quantitative analysis of the KF with sampling frequency equal to 140 kHz

Signals	Mean value of the Absolut values of the signals	Standard deviation	Maximum error
U_c [V]	8.0606	6.5281	64.0722
i_g [A]	6.9604	5.4948	45.5386

For plots in Fig. 7.11 and the discrete system dynamics with sampling frequency equal to 140 kHz and the weighting matrices are described as below:

$$A = \begin{pmatrix} 0.995 & -0.0460 & 0.0043 \\ 0.143 & 0.9867 & -0.1437 \\ 0.0128 & 0.1379 & 0.9859 \end{pmatrix},$$

$$B_1 = \begin{pmatrix} 0.0462 \\ 0.0033 \\ 0.0002 \end{pmatrix},$$

$$B_2 = \begin{pmatrix} -0.0002 \\ 0.010 \\ -0.1381 \end{pmatrix},$$

$$C_d = (1 \ 0 \ 0)$$

Measurement disturbances: $R = 1$

The process disturbance: $Q = \text{diag}([1 \ 0 \ 1])$

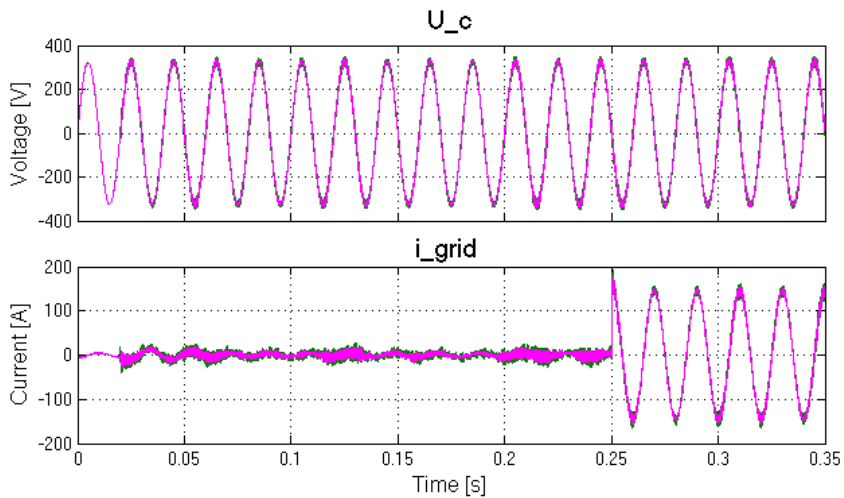


Fig. 7.11 Two plots on top are: capacitance voltage (pink) and estimated capacitance voltage (green), grid current (pink) and estimated grid current (green) for the KF for with sampling frequency = 140 kHz

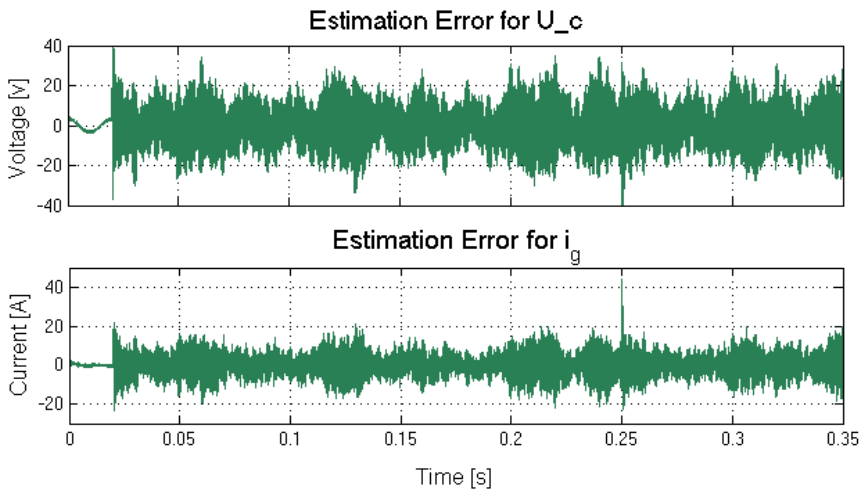


Fig. 7.12 The estimation error for the capacitance voltage (top) and for the grid current (bottom)

Table 7.4 The quantitative analysis of the KF with sampling frequency equal to 140 kHz

Signals	Mean value of the Absolute values of the signals	Standard deviation	Maximum error
U_c [V]	7.9393	6.1763518	59.9393
i_g [A]	5.3901	4.335787	47.7983

By comparing the Table. 7.3 and 7.4, one can see that the KF with higher sampling frequency gives a more accurate estimation of both signals

7.3 Simulation for Nonlinear System Dynamics

In this section the inductors in the line filter have been replaced by the designed nonlinear inductors in Matlab/Simulink in order to study the behavior of the system with this nonlinearity and then design a scheduled observer and the scheduled KF to estimate the desired signals. The effect of sampling frequency is studied in each design.

The nonlinear system in this case is described as:

$$\frac{d}{dt} \underbrace{\begin{pmatrix} i_1 \\ U_c \\ i_g \end{pmatrix}}_x = \underbrace{\begin{pmatrix} -\frac{R_1+R_c}{L_1(i)} & -\frac{1}{L_1(i)} & \frac{R_c}{L_1(i)} \\ \frac{1}{C} & 0 & -\frac{1}{C} \\ \frac{R_c}{L_2(i)} & \frac{1}{L_2(i)} & -\frac{R_2+R_c}{L_2(i)} \end{pmatrix}}_A \begin{pmatrix} i_1 \\ U_c \\ i_g \end{pmatrix} + \underbrace{\begin{pmatrix} \frac{1}{L_1(i)} \\ 0 \\ 0 \end{pmatrix}}_{B1} u_{inv} + \underbrace{\begin{pmatrix} 0 \\ 0 \\ -1 \\ \frac{1}{L_2(i)} \end{pmatrix}}_{B2} u_g$$

$$y = \underbrace{(1 \ 0 \ 0)}_C \begin{pmatrix} i_1 \\ U_c \\ i_g \end{pmatrix}$$

Observers/KF Scheduling

The observer Scheduling theory has been described in the previous chapter. In this section two different scheduling methods have been investigated and the results are shown and compared. Since the high sampling frequency has been investigated in the previous sub-section and it gave a better result. Below the

scenarios have been simulated with high sampling frequency ($f_s = 140$ kHz). The scheduling has been done by using the measurement signal (i_1).

- Scenario 1, three parallel observers for a nonlinear system are designed using the pole placement method
- Scenario 2, three parallel KF for a nonlinear system are designed solving the Riccati equation

Scenario 1, Estimation of Signals in the Nonlinear System by Using the Scheduled Observer

The signals were estimated by the observer and compared. The system dynamics for each observer are shown in Appendix B. The poles for each observer are placed as:

$$P1 = (0.7165 + 0.0000i, -0.3113 - 0.0058i, -0.3113 + 0.0058i)$$

$$P2 = (0.3520 - 0.7768i, 0.3520 + 0.7768i, 0.9582 + 0.0000i)$$

$$P3 = (0.2705 + 0.4764i, 0.2705 - 0.4764i, 0.8508 + 0.0000i)$$

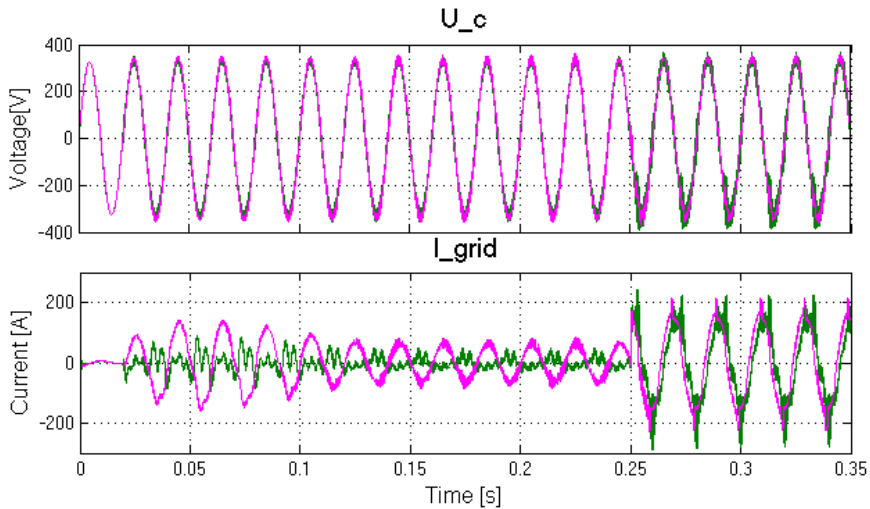


Fig. 7.13 The plot on top shows both the estimated u_c (pink) and the measured u_c (green) in the nonlinear system. The plot below shows the estimated i_g (pink) and the measured i_g (green) in the nonlinear system

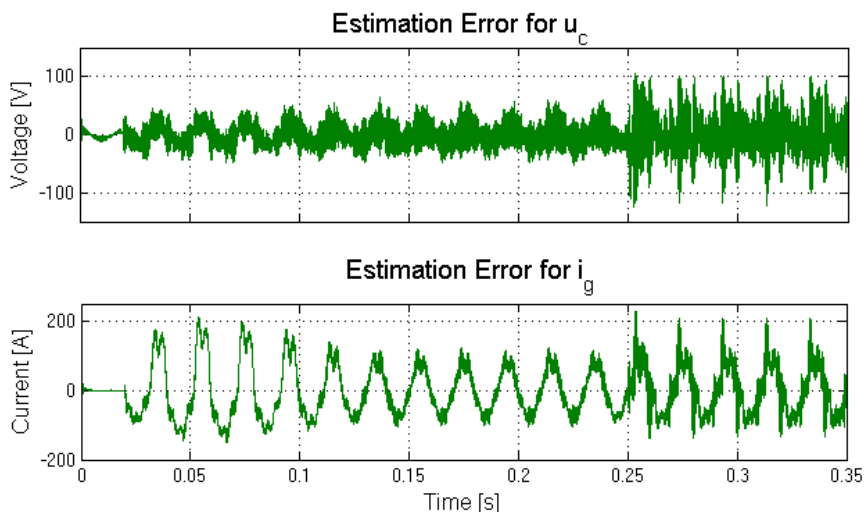


Fig 7.14 The scheduled observer estimation error for the capacitance voltage (top) and for the grid current (bottom)

Table 7.5 The quantitative analysis of the Scheduled observer error with sampling frequency equal to 140 kHz

Signals	Mean value of the Absolute values of the signals	Standard deviation	Maximum error
U_c [V]	17.2768	14.8262	124.3164
i_g [A]	61.5416	40.8865	229.6074

Result: as one can see the ground tone is closely followed by the estimator. The estimator can't follow the high frequent ripple exactly. The estimation error for ripple current and voltage is quite high because the nonlinearity of the inductors affects the switching ripple directly by not damping them.

Scenario 2, Estimation of signals in the Nonlinear System by Using the Scheduled KF

The objective of this simulation is to show the performance of scheduled KF for two different weighting matrices. Figures 7.15-16 show the result for the scheduled KF with $Q = \text{diag}([1 \ 1 \ 1])$ and $R = 1$.

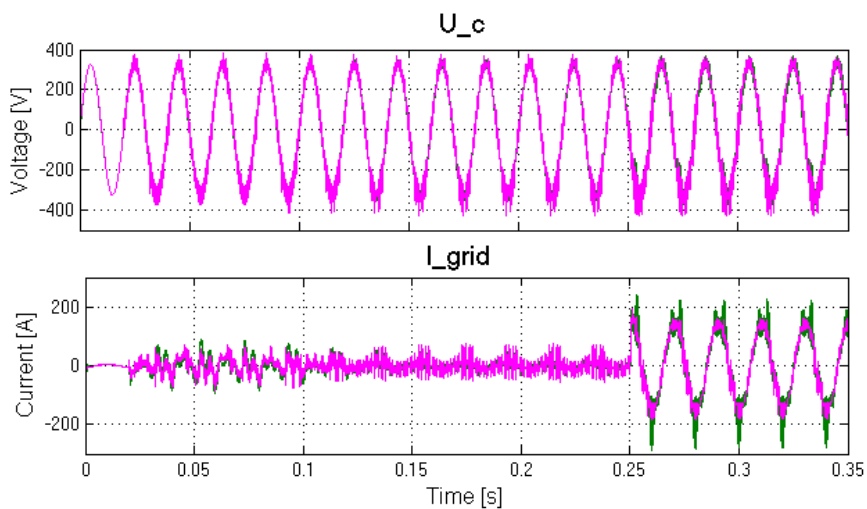


Fig.7.15 The plot on top shows both the estimated u_c (pink) and the measured u_c (green) in the nonlinear system. The plot on bottom shows the estimated i_g and the measured i_g in the nonlinear system

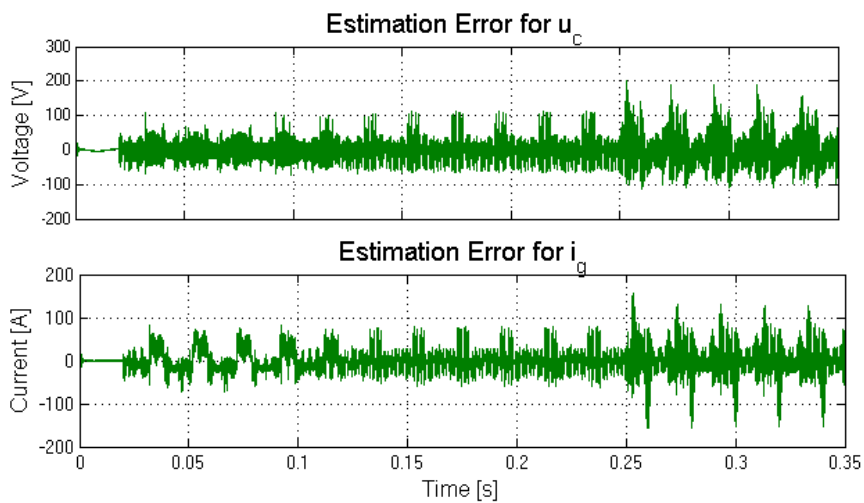


Fig. 7.16 The scheduled KF estimation error for the capacitance voltage (top) and for the grid current (bottom)

Table 7.6 The quantitative analysis of the Scheduled KF error with sampling frequency equal to 140 kHz

Signals	Mean value of the Absolut values of the signals	Standard deviation	Maximum error
U_c [V]	24.2478	21.6220	200.5603
i_g [A]	18.9009	18.8269	155.1762

Figures 7.17-18 show the result for the scheduled KF with $Q = \text{diag}([1 \ 1 \ 2])$ and $R = 10$

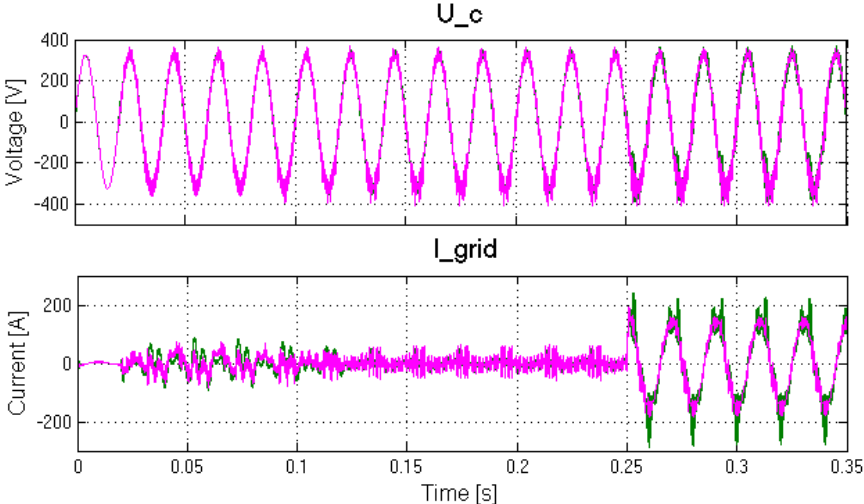


Fig. 7.17 The plot on top shows both the estimated u_c (pink) and the measured u_c (green) in the nonlinear system. The plot on bottom shows the estimated i_g and the measured i_g in the nonlinear system

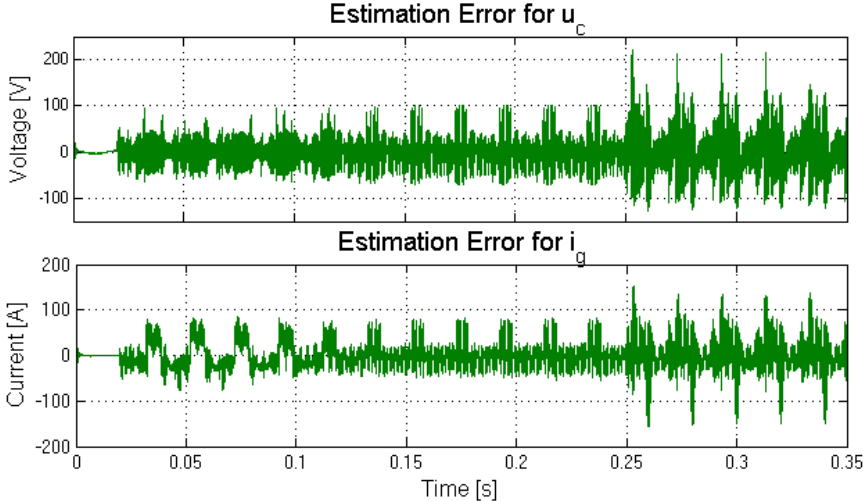


Fig. 7.18 The estimation error for the capacitance voltage (top) and for the grid current (bottom)

Table 7.7 The quantitative analysis of the Scheduled KF error with sampling frequency equal to 140 kHz

Signals	Mean value of the Absolut values of the signals	Standard deviation	Maximum error
U_c [V]	23.6893	22.2021	124.315
i_g [A]	20.2223	19.8116	153.3619

By introducing some model error (is described in subsection under title” Case 2, Estimation of Signals in the Nonlinear System by Using the Scheduled Kalman Filter”) we see that the KFs produce usable estimates. The u_c signal will be used in the controller in an ADF and a better estimation of the u_c is obtained by scheduled KF with $Q = \text{diag}([1 \ 1 \ 2])$ and $R = 10$. The benefit of using KF is increased robustness of feedback control at sensor failure.

Discussion, Future works and Recommendations

By comparing the plots that are shown in this chapter, I can show that a better estimation of signals will be obtained by having higher sampling frequency. A better performance is obtained when the KF with high sampling frequency is applied on the system. Another main conclusion is that estimating continuous-time system by using sampled observers requires more care about how to choose sampling method. The ripple current and voltage on the signals have very high frequency and high amplitude. The ripple amplitude in the nonlinear system became somehow more than twice the ripple amplitude in the linear system (see Fig. 5.4). The result of this observer scheduling method that I used in this thesis to overcome the nonlinearity are presented in the previous subsection. They indicate that the design method is not well suited for these high frequent ripples. However, it is up to Comsys AB to decide how to use the result. Additional studies are needed, before Comsys AB use the result in ADFs control loop.

There are many publications that describe line filter performances from different aspects (i.e. [5]), but there is almost no literature that describe the effect of nonlinear inductors in the line filter. The focus in this thesis was mainly on the nonlinearities due to the non-ideal inductors in the line filter. The simulated model of the LCL filter was connected to the simulated converter with high switch. The switching frequency has an influence on the current harmonics distortions and the losses in the line filter inductors, especially on the L_1 [5, 43]. The resonance

frequency of the system (see Bode diagrams in the chapter 2 and 3) will change since the inductances for L_1 and L_2 are changed. Different resonance frequencies will give different bandwidths for the system. The change of the bandwidth will lead to a poor dynamic performance of the control system [43]. As it is shown in Fig. 3.5 the decrease of the inductance value will lead to the improving of the bandwidth and thereafter a better system dynamics but the attenuation of the current ripple will decline. Figures 5.6-7 show how the current ripple will be at least twice as high when the inductances decrease only by 20%. There must be other publications that study these nonlinearities but in this work they were not considered, consequently, the designed observer for the nonlinear LCL filter does not estimate these nonlinearities. Advanced system identification is required in order to configure the behavior of the system when it is connected to the other part of the ADF system as well as to be able to study the disturbances and the noise in the line filter. An extended Kalman filter (EKF) may give better result but in order to implement the EKF Comsys need to study the mathematical relationship between the inductance and the current for the inductors. A scheduled observer has been applied and the result has been presented in this work. Depending on what is required of the estimator (to estimate the ground tone or estimate the ripple currents and voltage) this solution can work well.

Validity

I haven't been able to find research publications concerned with line filters that take non-linearity of inductors into account. Therefore it isn't possible to validate and support the results by comparison with results from similar projects. Since running the line filter model was totally depended on the others parts of the Simulink model for ADF and since studying the other parts of the ADF was outside of the thesis scope, the result might be affected by some other parameters. For example there were some "sample and hold" blocks in the control part of the Simulink model and the observers are placed in the same block as the controller model which means that the observers will be affected by delay that is caused by the "sample and hold" blocks.

8. References

- [1] G. Shen, X. Zhu, J. Zhang, and D. Xu, A New Feedback Method for PR Current Control of LCL Filter-Based Grid-Connected Inverter, Industrial Electronics, February 2010 IEEE Transactions on (Volume:57, Issue:6), pp 2033 – 2041
- [2] <http://en.wikipedia.org/wiki/Inductor>
- [3] T. Hägglund, Reglerteknik AK, Department of Automatic Control, Lund University 2011, Sweden
- [4] K-E. Årzen, Real-time control systems part 2, Department of Automatic Control, Lund University 2012, Sweden
- [5] M. Lindgren, Modeling and Control of Voltage Source Converters Connected to the Grid, Ph.D. Thesis No. 351, Chalmers University, Department of Electric Power Engineering, Sweden, November 1998
- [6] S. Sharoffa.M and C. Sumathy.A, A Low Cost Fly back Continuous Conduction Mode Inverter With LCL Filter For Ac Module Application, IOSR Journal of Engineering (IOSRJEN) Vol. 3, Issue 6 , PP 14 – 18 , June. 2013
- [7] M. Liserre, A. Dell’Aquila, F. Blaabjerg, Stability Improvements of an LCL filter Based Three-phase Active Rectifier, Power Electronics Specialists Conference (PESC), 2002 IEEE 33rd Annual Vol.3, pp 1195 – 1201,
- [8] B. Bolsens, K. De Brabandere, J. Van den Keybus, J. Driesen and R. Belmans, Model-Based Generation of Low Distortion Currents in Grid-Coupled PWM-

Inverters Using an LCL Output Filter, Power Electronics Specialists Conference (PESC) 04. 2004 IEEE 35th Annual Vol.6, pp 4616 – 4622

[9] S. Cobreces¹, E. Bueno¹, F. J. Rodriguez¹, F. Huerta¹, P. Rodriguez, Influence Analysis of the Effects of an Inductive-Resistive Weak Grid over L and LCL Filter Current Hysteresis Controller, 2007 Power Electronics and Applications, IEEE, Aalborg, September 2-5, 2007 , pp 1– 10

[10] S. J. Julier and J. K. Uhlmann, New extension of the Kalman filter to nonlinear systems, Signal Processing, Sensor Fusion, and Target Recognition conference VI, Proc. SPIE 3068, Orlando, FL, USA, April 21, 1997

[11] B. Ristic, S. Arulampalam, N. Gordon, Beyond the Kalman Filter particle filters for tracking applications, Artech House, London, 2004

[12] E. A. Wan and R. van der Merve, The Unscented Kalman Filter for Nonlinear Estimation, Adaptive Systems for Signal Processing, Communications, and Control Symposium 2000 AS-SPCC, 2000 IEEE, Lake Louise, Alta, October 1- 4, 2000, pp 153 –158

[13] A. Pellett, The extended Kalman-Consensus filter, Master Thesis, Department of Computer Engineering, The University of Maine, Paper 1593, December 2011

[14] State estimation with Kalman filter chapter 18,
http://home.hit.no/~hansha/documents/control/theory/stateestimation_with_kalmanfilter.pdf

[15] M. Zheng, K. Ikeda and T. Shimomura, Estimation of Continuous-Time Nonlinear Systems by Using Unscented Kalman Filter, SICE Annual Conference, Japan, May 1, 2010, Vedran Kordic (Ed.).

[16] S. Pettersson, M. Salo and H. Tuusa, Applying an LCL filter to a four-wire active power filter; 37th Power Electronics Specialists Conference (PESC 2006), Jeju, June 18 – 22, 2006, pp 1-7

[17] R. Johansson, Predictive and Adaptive Control, Department of Automatic Control, Lund University, 2008

- [18] M. Ciobotaru, Reliable grid condition detection and control single-phase distributed power Generation Systems, Ph.D. thesis No. DK-9220, Faculty of Engineering, Science & Medicine at Aalborg University, ISBN :978-87-89179-77-3, January 2009
- [19] R. A. Mastromauro, M. Liserre and A. Dell'Aquila, Study of the Effects of Inductor Nonlinear Behavior on the Performance of Current Controllers for Single-Phase PV Grid Converters, Industrial Electronics, IEEE Transactions on Vol. 55, Issue: 5, April 30, 2008, pp 2043 – 2052
- [20] D. H. Boteler, Characteristics of Time-Varying Inductance, IEEE Transactions on Magnetics, Volume: 30, Issue: 2, August 06, 2002, pp 172 – 176
- [21] Huerta.F, Bueno.E, Cobreces.S, Rodriguez. F.J and Giron.C, Control of grid-connected voltage source converters with LCL filter using a Linear Quadratic servo controller with state estimator, 2008 IEEE, Power Electronics Specialists Conference (PESC 2008), Rhodes, June 15-19, 2008, pp 3794 – 3800
- [22] M. Bojrup, Advanced Control of Active Filters in a Battery Charger Application, Ph.D. Thesis No. S-221 00, Department of Industrial Electrical Engineering and Automation, Lund University, Sweden, 1999
- [23] W. Yu, Optimization of Spiral Inductors and LC Resonators Exploiting Space Mapping Technology, Master thesis, Department of Electrical and Computer Engineering, McMaster University, Hamilton, Ontario, June 2006
- [24] G. Liu and X.B. Xu, Improved Modeling of the Nonlinear B-H Curve and Its Application in Power Cable Analysis, Magnetics, 2002 IEEE Transactions on Volume:38, Issue: 4, August 07, 2002, pp 1759 – 1763
- [25] M. Vakilian and R. C. Degeneff, A Method for Modeling Nonlinear Core Characteristics of Transformers During Transients, Power Delivery, IEEE Transactions on Vol. 9, Issue: 4, Oct 1994, pp 1916-1925
- [26] Matlab toolbox for inductor,
<http://www.mathworks.se/help/physmod/elec/examples/nonlinear-inductor-characteristics.html>

- [27] W. Sun, X. China, Z. Chen, X. Wu, Intelligent optimize design of LCL filter for three-phase voltage-source PWM rectifier, Power Electronics and Motion Control Conference (IPEMC 2009), 2009 IEEE 6th International, Wuhan, May17-20 2009, pp 970 – 974
- [28] P. Cortés, G. Ortiz, J. I. Yuz, J. Rodríguez, S. Vazquez and L. G. Franquelo, Model Predictive Control of an Inverter With Output LC Filter for UPS Applications, 2009 IEEE Transactions on Industrial Electronics, (Volume:56, Issue: 6), June 2009, pp 1875-1883
- [29] N. Hoffmann, M. Hempel, M.C. Harke and F.W. Fuchs, Observer-based grid voltage disturbance rejection for grid connected voltage source PWM converters with line side LCL filters, 2012 IEEE Energy Conversion Congress and Exposition (ECCE), September 15 – 20, 2012, Raleigh, NC, pp 69 – 76
- [30] T. Glad and L. Ljung. reglerteori. Flervariabla och olinjära metoder, Studentlitteratur, Lund, Sweden, 1997
- [31] B. K. Aliyu, Charles A. Osheku, Lanre M.A. Adetoro and Aliyu A. Funmilayo, Optimal Solution to Matrix Riccati Equation – For Kalman Filter Implementation, MATLAB - A Fundamental Tool for Scientific Computing and Engineering Applications - Volume 3, Prof. Vasilios Katsikis (Ed)(2012).
- [32] M. Djerf, Power grid integration using Kalman filtering, Master thesis No. E12003, Department of Engineering Sciences, Signals and Systems Group Uppsala University, Sweden, February 2012
- [33] L. Glielmo, P. Marino, R. Setola, F. Vasca, Parallel Kalman filter algorithm for state estimation in bilinear system, Decision and Control, 1994., Proceedings of the 33rd IEEE Conference on (Volume:2), Lake Buena Vista, FL, December 14 - 16, 1994, pp 1228 – 1229
- [34] S.C Chung, S.R Huang, J.S Huang and E.C Lee, Applications of describing functions to estimate the performance of nonlinear inductance, Science, Measurement and Technology, IEEE Proceedings, (Volume:148, Issue:3), May 2001, pp 108 – 114

- [35] E. Hansson and M. Sträng, Design and evaluation of a distributed control architecture over switched Ethernet in active filters, Master thesis No. TFRT-5878, Department of Automatic control, Lund University, Sweden, March 2011
- [36] R. Johansson, System Modeling and Identification, Prentice Hall, Englewood Cliffs, New Jersey, 1993, pp 512
- [37] Y. Liu, Robust Nonlinear Control Design with Proportional-Integral-Observer Technique, Ph.D. Thesis, Document No. 25392, January 2011, Duisburg-Essen University, Germany
- [38] M. Liserre, F. Blaabjerg, and S. Hansen, Design and Control of an LCL Filter-Based Three-Phase Active Rectifier, IEEE Transactions on Industry Applications Vol. 41, Issue:5, October 2005, pp 1281-1291
- [39] J. Svensson, Grid-connected voltage source converter-control principles and wind energy applications, Ph.D. Thesis No. 331, Department of electric power engineering, Chalmers University of technology, Sweden, 1998
- [40] K. Svartveit, Attitude determination of the NCUBE satellite, Master thesis, Department of Engineering Cybernetics, NTNU, Trondheim Norway, June 2003
- [41] L. Kleeman, Understanding and Applying Kalman Filtering, Department of Electrical and Computer Systems Engineering, Monash University, Clayton, http://www.cs.cmu.edu/~motionplanning/papers/sbp_papers/integrated3/kleeman_kalman_basics.pdf
- [42] Wikipedia, http://en.wikipedia.org/wiki/Jacobian_matrix_and_determinant
- [43] X. Shi, Z. Wang, Y. Ma, L. Hang, L.M. Tolbert, and F. Wang, Modeling and Control of an LCL Filter Based Three-phase Active Rectifier in Grid Emulator, 2013 28th IEEE Power Electronics Conference and Exposition (APEC 2013), Long Beach, CA, March 17 – 21, 2013, pp 992-998

Appendix A

The information of the filter capacitor voltages and grid currents are needed in the purpose of the reducing the number of the sensor.

An illustration of how the KF was implemented in Simulink is shown in Fig. (6.2)

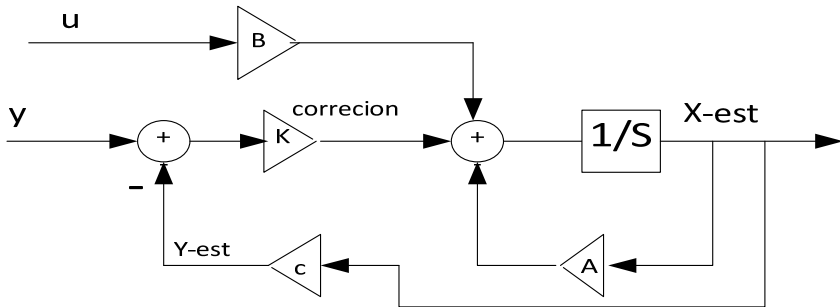


Fig. 8.1 Implementation of the continues-time KF in Simulink

Appendix B

Matlab code for embedded Scheduled KF

```
function xhatout = kalmanfilter(i_con,u_g,u_inv)

persistent xhat Ad Bd Cd p1 Kg Ad1 Ad2 Bd1 Bd2 Kg1
Kg2 p p2 p3 Q R

if isempty(p)

    xhat = zeros(3,1);
    Ad= [-(R_C1+R_L1)/L1 -1/L1 R_C1/L1; 1/C1 0 -
    1/C1;R_C1/L2 1/L2 -(R_C1+R_L2)/L2];

    Ad1= [-(R_C1+R_L1)/L1K1 -1/L1K1 R_C1/L1K1; 1/C1 0 -
    1/C1;R_C1/L2K1 1/L2K1 -(R_C1+R_L2)/L2K1];

    Ad2= [-(R_C1+R_L1)/L1K2 -1/L1K2 R_C1/L1K2; 1/C1 0 -
    1/C1;R_C1/L2K2 1/L2K2 -(R_C1+R_L2)/L2K2];
```

```

B1= [1/L1;0;0];
B2= [0 ;0; -1/L2];
Bd= [B1 B2];
Bd1=[1/L1K1 0; 0 0 ;0 -1/L2K1];
Bd2=[1/L1K2 0; 0 0 ;0 -1/L2K2];

Cd = [1 0 0];
p1 = zeros(3);
p3 = zeros(3);
p2 = zeros(3);
Q = 1*eye(3);
R = 10;

end
p=1;

if abs(i_con)>=0  &&  abs(i_con) <= 50

    xhat = Ad*xhat+ Bd(:,1)*u_inv + Bd(:,2)*u_g;
    p1 = Ad*p1*Ad'+ Q;
    Kg = p1*Cd' / (Cd*p1*Cd'+R);
    resid = i_con - Cd*xhat;
    xhat = xhat + Kg*resid;
    p1 = (eye (size(Kg,1))- Kg*Cd)*p1;

elseif abs(i_con)>50  &&  abs(i_con) < 150

    xhat = Ad1*xhat+ Bd1(:,1)*u_inv + Bd1(:,2)*u_g;
    p2 = Ad1*p1*Ad1'+Q;
    Kg1 = p2*Cd' / (Cd*p1*Cd'+R);
    resid = i_con - Cd*xhat;
    xhat = xhat + Kg1*resid;
    p2 = (eye (size (Kg1,1))- Kg1*Cd)*p2;

else abs(i_con)>= 150  &&  abs(i_con) < 190

    xhat = Ad2*xhat+ Bd2(:,1)*u_inv + Bd2(:,2)*u_g;
    p3 = Ad2*p3*Ad2'+Q;
    Kg2 = p3*Cd' / (Cd*p3*Cd'+R);
    resid = i_con - Cd*xhat;
    xhat = xhat + Kg2*resid;
    p3 = (eye (size (Kg2, 1)) - Kg2*Cd)*p3;

```

```
end
xhatout = xhat;
```

Matlab Code for the Observer

```
A = [-(R_C1+R_L1)/L1 -1/L1 R_C1/L1; 1/C1 0 -
1/C1;R_C1/L2 1/L2 -(R_C1+R_L2)/L2];
B1= [1/L1;0;0 ];
B2= [0 ;0; -1/L2];
B = [B1 B2 ];
C = [1 0 0];
D = 0;
fs=2*7200;
ts=1/fs;
t_sim=ts/100;
Ts_FPGA_Speed = t_sim;

%system description-----

Plant =ss(A,B ,C,D);
[sysd] = c2d(Plant,ts);
Cd=sysd.c;
Bd=sysd.b;
Ad=sysd.a;
SystemContinusPoles = eig(A);
eig(Ad);
POlesPlacering = exp(SystemContinusPoles.*36*ts);
K = acker(sysd.a',sysd.c',POlesPlacering)';
```


Lund University Department of Automatic Control Box 118 SE-221 00 Lund Sweden		<i>Document name</i> MASTER 'S THESIS	
		<i>Date of issue</i> April 2014	
		<i>Document Number</i> ISRN LUTFD2/TFRT--5938--SE	
<i>Author(s)</i> Taravat Saryan		<i>Supervisor</i> Nils Lundström, Comsys AB Rolf Johansson, Dept. of Automatic Control, Lund University, Sweden (examiner)	
		<i>Sponsoring organization</i>	
<i>Title and subtitle</i> Modeling and Observer Design of a Nonlinear LCL Filter for Three- Phase Grid-Connected Voltage Source Converter			
<i>Abstract</i> <p>This work presents an observer design for grid current and capacitor voltage of voltage source pulse-width modulation (PWM) converters with LCL filter. Theoretical aspects including the mathematical LCL filter system observability, observer placement strategy and practical discretization implementation. It gives insight to mathematical modelling of the line filters dynamics. By the limitations of how the components in the line filter operates, the Kalman filter is adjusted accordingly.</p> <p>The strategy for designing the Kalman filter is presented. A time-varying KF is developed, benchmarked and implemented in simulator.</p> <p>Through an explanation of the magnetic field fundamentals, a nonlinear model of the inductors is modeled and used. An observer scheduling development has been implemented on the nonlinear system. The effect of sampling frequency is studied for KF and for the observer as well. At last the results are presented and analyzed.</p>			
<i>Keywords</i>			
<i>Classification system and/or index terms (if any)</i>			
<i>Supplementary bibliographical information</i>			
<i>ISSN and key title</i> 0280-5316			<i>ISBN</i>
<i>Language</i> English	<i>Number of pages</i> 1-71	<i>Recipient's notes</i>	
<i>Security classification</i>			